N68-14579

Grumman Research Department Report RE-311

DETERMINATION OF THE COEFFICIENT OF FRICTION BETWEEN METALS AND NONMETALS IN ULTRAHIGH VACUUM

by

G. Mohr

and

L. L. Karafiath

Geo-Astrophysics Section

December 1967

Final Report

on

Contract No. NAS 8-5415

Project 0284

Prepared for
National Aeronautics and Space Administration
George C. Marshall Space Flight Center
Huntsville, Alabama

Approved by: Charles E. Mack, Jr.
Director of Research

FOREWORD

The work reported herein was performed in the Geo-Astrophysics Section of the Research Department with J. D. Halajian (Advanced Systems) principal investigator, G. Mohr in charge of the experimental work, and L. L. Karafiath participating in the soil mechanics evaluation of the experiments. The instrumentation was designed by F. J. Meinhart (Corporate Instrumentation and Data Processing Services). Computer analysis of the data was performed in the Data Processing Department under the direction of H. Turner.

The ultrahigh vacuum chamber and the friction testing apparatus were manufactured in the machine shop of the Research Department; commercially available components were used where possible. S. Mole of the Welding Department performed the difficult task of welding the vacuum chamber and other components of the system. G. Homfeld assisted in the operation of the vacuum system and in the performance of tests.

ABSTRACT

This report is in partial fulfillment of the reporting requirements of Contract NAS 8-5415, the "Determination of the Coefficient of Friction Between Metals and Nonmetals in Ultrahigh Vacuum," and is the final report for Modification 3 of that contract. During the contract period, 20 friction tests at pressures below 2×10^{-9} torr were performed; in 19 of the vacuum tests, the pressures were in the 10^{-10} torr range or lower. In addition to these tests in vacuum, supplemental tests under atmospheric conditions were conducted for the purpose of comparison. The test temperature was the same in all cases, normal room temperature between 20 and 25°C, with a relative humidity controlled at about 35 percent. Friction between basalt and quartz powders (in two particle size range, 250-500 microns and 38-62 microns) and metal disks (steel 1020 and aluminum 7075) were measured under these two conditions.

Computer programs based on the least squares method were used to obtain best fitting first and third order curves. The digitalized data as well as the best fit curves were then plotted on a greatly magnified scale. Typical example of plots so prepared are presented. Illustrations and photographs showing the friction measuring arrangement, the vacuum system, strain gauge calibration procedures, outgassing rates of basalt and quartz powders, pressure evolution curves, and other pertinent documentation are also included in the appropriate sections of this report.

The observed values of the coefficient of friction followed the same pattern in all of the tests. From an initially high value, designated μ_i, the coefficient of friction declined rapidly with time until it reached a nearly constant value of kinetic friction, designated μ_c. The initial value μ_i was only slightly higher than μ_c, for the tests performed in air, but in most tests performed in ultrahigh vacuum, μ_i was significantly higher than μ_c. If for each set of tests, the ratio

$$\mu_i \text{ (vacuum)} / \mu_i \text{ (air)}$$

is formed, it is found to be greater than 1 in all cases except for steel 1020 sliding on fine quartz powders. For almost all tests this ratio is much higher than the corresponding ratio

$$\mu_c \text{ (vacuum)} / \mu_c \text{ (air)} .$$

Except for two cases, this latter ratio shows the same general tendency, but in a less pronounced manner. Ratios higher than 1.5 are more typical for μ_i (vacuum)/μ_i (air); ratios in the range of 1.1-1.2 are typical for μ_c (vacuum)/μ_c (air).

These experiments have proven conclusively that very low pressures affect the frictional behavior of dissimilar materials. For most combinations of the materials tested, it has been established that the coefficient of friction between metals and granular soils increases considerably under the influence of very high vacua. The variations in the measured values of the coefficients of friction indicate a dependency on surface conditions, the forces applied, and the ratio of the metal-soil friction to the internal friction of the soils.

TABLE OF CONTENTS

LIST OF ILLUSTRATIONS

LIST OF TABLES

I. INTRODUCTION

This report discusses the analytical and experimental investigations used to determine the coefficient of friction between various metal surfaces and various, granular soil-like nonmetals in an ultrahigh vacuum environment. These investigations, which have been conducted at Grumman under the sponsorship of the Marshall Flight Center, NASA Contract 5415, since 1964, are aimed at the better understanding of frictional phenomena in ultrahigh vacuum. They further serve the purpose of obtaining quantitative values for the coefficient of friction between metals and soils needed for the design of lunar landing and roving vehicles.

Specifically, the work includes, according to contract stipulations:

A. A series of measurements made in accordance with the following conditions.

   1. The vacuum shall be 10^{-9} torr or greater. Vacuum shall be the only variable required during the tests. Tests shall include 20 separate pumpdowns. The samples shall be at ambient temperature when the data are taken.

   2. The nonmetallic samples will consist of basalt and quartz with particle sizes of 0.25 to 0.50 mm and 0.038 to 0.062 mm. Each test will be made with a fresh sample.

   3. The metal sliders will be made of aluminum 7075 and steel AISI 1020; a fresh slider will be used for each test.

   4. The load on the test mechanism shall be kept constant during a set of tests in air and ultrahigh vacuum.

   5. There will be at least two tests on each nonmetallic sample size with the same type metal slider.

B. For each vacuum test, there will be a corresponding air test to allow a determination of the effect of vacuum on the coefficient of friction.

C. Following a series of air/vacuum tests performed to determine the influence of vacuum alone on the measurements, other variables such as temperature or load may be introduced.

The granular materials, basalt and quartz, and the specific particle sizes had been chosen because of their widespread use in lunar surface simulation studies. The choice of the materials for the metal disks was motivated by their importance for engineering applications in the development of space vehicles. The specimens were prepared so that they would be compatible with ultrahigh vacuum techniques. No effort was made to produce atomically clean surfaces by electron bombardment, ion sputtering or similar methods. Outgassing of the vacuum system, including the specimens, was always achieved with normal baking temperatures, which never exceeded 210°C at the chamber or 400°C at the pumping section of the system. In order to assure the highest possible vacuum, a new test fixture and instrumentation, made of materials and components that are compatible with the most stringent requirements of ultrahigh vacuum technology, had to be designed and constructed for this latest phase of this program. These will be described in detail in Section II.

During the first 16 tests, exposure of the specimens to very low pressures was relatively brief (see Section II-C). It was, therefore, of importance to evaluate the influence of much longer periods of vacuum exposure on the coefficient of friction. Consequently, during two of the tests stipulated under part C of the contract, as noted above, the specimens were exposed to pressures below 1×10^{-9} torr for a period of ten days. In addition, at the end of the eighth day, the metal disk was lowered onto the powder and the load applied. The setup then remained in this condition until the coefficient of friction was measured at the end of the tenth day. In the remaining two tests, the changed variables were load and speed of rotation, respectively.

II. TEST EQUIPMENT DESIGN

A. Testing Apparatus

Figure 1 shows the friction measuring apparatus used in the experiments. It underwent several modifications before repeatable results became feasible. The original bellows assembly on top of the vacuum chamber for load application was replaced by a direct loading assembly to permit weights to be placed and held in position above the metal disk holder. The whole assembly is free to move up and down so that the test surfaces can be separated during outgassing of the system. In this arrangement, the applied normal load is constant and known, and cannot change during rotation by the contraction or expansion of the bellows. The function of the bellows has been reduced to that of a positioning device.

The platform supporting the granular specimens container and the shaft linking it to the strain gauge balance were made of boron-nitride, an insulator, in order to reduce heat flow toward the strain gauges. Separate heating elements, connected to an external high current-low voltage power source, permit selective outgassing of either the metal disk or the mineral powder, or both specimens simultaneously. For measurements at room temperature, however, normal outgassing procedures of the whole system have been found satisfactory to reach the desired ultimate pressures, after pretreating the powders as described in Section III.

Spun stainless steel cups were used to contain the granular specimens. The cups were 2-3/8" in diameter and 3/4" deep; their upper edge was bent outward to prevent friction between the outer rim of the disk and the powder. The weights of the granular specimens were kept constant throughout the tests: 65.6 gr for coarse and fine basalt and coarse quartz, 53.6 gr for fine quartz.

The diameter of the metallic disks used in the investigation was 1-1/2", and their cross-sectional thickness approximately 0.025". They were formed by spinning, and finished by grinding and polishing to a finish of less than 6 microinches (rms). Shortly before a test or pump-down, the carefully cleaned disk was fastened to the disk holder, and a specified quantity of mineral powder was placed inside the sample container. The granular specimen container and the disk holder were easily accessible by removal of the large viewing port in front of the vacuum chamber (see Fig. 2).

The rotating section of the friction measuring unit is driven by a small, variable speed, dc servo motor (Fig. 3). Mounted on a support bracket, which in turn is joined to a rigid U-frame by means of a threaded connection, the motor can be lowered and raised within a fixed distance. During baking of the system, the motor support bracket is removed from the top of the rotary feedthrough flange. For transmission of motion into the vacuum chamber, a flexible coupling connects the motor drive shaft to the input shaft of a NRC-rotary harmonic feedthrough. This feedthrough is a positive drive type device that is compatible with ultrahigh vacuum requirements in all respects.

B. Instrumentation

The strain gauge balance was fabricated from a custom built forging (see Figs. 4 and 5). A diaphragm section about the center of the unit is instrumented to measure axial loads; a thin-walled vertical cylindrical member is instrumented to measure the torsional forces. Normal forces are measured by means of a two-active arm bridge; torsional forces by means of a four-active arm bridge. Both measuring circuits use semiconductor strain gauges. The range of load calibration was ±32 inch-ounces of torsion in increments of 3 inch-ounces, and a 5 lb axial load in increments of 1/4 lb.

The sensitivity of the strain gauge circuits can be influenced in several ways, and these may give rise to slight errors in the measurements. There is a shift in "zero-output" of the torsion circuit of approximately 0.32 inch-ounces for each pound of normal force applied. This, however, will not affect the torsion circuit calibration if the normal force remains constant during a run. If the total normal force vector acting on the cup varies in position during a run, it will apply a bending moment to the torsion member, thus causing an output error in the torsion circuit of as much as 0.026 inch-ounces of torque for each inch-ounce of bending moment applied to the torsion member. This error varies sinusoidally with the azimuth angle of the torsion column. The normal force circuit is also affected by the bending moments applied to the torsion column, and the output will vary if the normal force vector varies in position. Each inch-ounce of bending moment applied can cause an error of as much as 0.0056 lb in the normal force circuit output. During tests 1 through 34, the output from the strain gauge circuits was fed into a Brush Dual Gauge Amplifier with a Brush Recorder Mark II. During tests 35-40 a MASSA-COHU Recording Oscillograph and CARRIER amplifiers were used. For protection of the strain gauges during bake-out of the system, a water cooling groove was machined directly into the strain gauge balance.

C. Vacuum System

1. Components

The ultrahigh vacuum system (Figs. 6 and 7) used for the friction tests was specially designed and developed by Grumman for the study of friction between metals and soils under simulated lunar conditions. It consists of a working chamber, various pumps, a gas handling system, several different gauges, including a residual gas analyzer, electrical and instrumentation feedthroughs, and special heaters. For baking the whole system, a combination of ovens, heating strips and tapes, and baking mantles were available. The power input to all these heating components is individually controllable, thereby enabling the operator to bake only a specific section of the system when needed, or keep the various sections at varying temperature, or establish temperature gradients in any desired direction.

2. Pumping System

The pumping system was chosen so that we could obtain vacua as high and clean as the present state of the art permits when working with such gaseous materials as mineral powders. Pressures as low as 5×10^{-11} torr were routinely reached with the chamber clean and empty. With loads, ultimate pressures increased by less than one decade.

During the first six pump-downs, rough-pumping was achieved with three liquid nitrogen-cooled sorption pumps in series. Later, a Welch Turbo-Molecular pump with a pumping speed of 260 l/s and ultimate pressure capabilities in the low 10^{-8} torr range was added to the system for roughing and pumping during bake-outs. Toward the end of a baking cycle, all valves, one of them bakeable, connecting the system to the manifold of the turbomolecular pump are closed, and the ultrahigh vacuum pumps are turned on. At this point, the pressure has usually decreased to 10^{-7} torr or lower (see Fig. 8). The pressure is rapidly lowered further by a combination of an ion pump and a titanium sublimation pump with an estimated combined pumping speed of 700 l/s. Finally, when the pressure approaches an ultimate value that is typical for this system, a helium cryopump is activated, which ordinarily leads to an instantaneous drop in pressure of nearly half a decade.

III. TESTING PROCEDURES

A. Preparation of Soil Samples

1. Source of Material

Large quartz crystals from Hot Springs, Arkansas and chunks of basalt from Somerset County, New Jersey were comminuted and sifted by the procedure described in detail in Appendix A to obtain the following grain size ranges:

Material	Range of Particle Sizes
Coarse	250 - 500 microns
Fine	38 - 62 microns

2. Storage of Material

The granular material was generally stored in sealed glass jars; the material selected for testing was placed and stored in a separate vacuum chamber where it was baked and outgassed. Although the material was necessarily exposed to air again when it was placed in the sample container, this procedure reduced the outgassing time of the friction experiment.

3. Placement of Material in the Sample Container

The same weight of soil was used for one type of material in all the tests. The container was filled with the loose soil and carefully evened to the same level in each test with the help of an Airite vibrator. The following tabulation shows the weights used for each soil type, the specific gravity, the moisture content as stored, the dry density, and porosity of the soil.

Material	Size Range μ (microns)	Sample Weight g	Specific Gravity g/cm^3	Moisture Content %	Dry Density g/cm^3	Porosity %
Quartz	250-500	66	2.655	< 0.1	1.73	34.8
	38-62	54	2.662	< 0.1	1.42	46.8
Basalt	250-500	66	2.914	0.26	1.73	40.4
	38-62	66	2.990	0.7	1.72	42.5

Note that despite the great care taken to ensure uniform preparation of the specimens, uncontrolled differential gas pressures were inadvertently generated between the chamber and the inside of the specimens during baking and pump-down. These differential pressures tended to loosen the specimen, and in some instances resulted in minute craters on the surface.

B. Preparation of Metal Disks

1. Polishing

Upon completion of machining operations, all metal disks are checked for concentricity before polishing. Only disks with a total run-out of less than .003" are accepted for further processing. Polishing is accomplished in four distinct steps:

1) Dry-polish with 400 grid silicone paper,
2) Dry-polish with 600 grid silicone paper,
3) Wet-polish with 210 emery paper, and
4) Wet-polish with 410 emery paper.

For wet polishing, ordinary, undiluted, soluble, machining oil is used. The polished disks are once more checked for concentricity, and their degree of finish is measured with a profilometer. If the measured value is below 6 microinches (rms), it is marked on the back of the disk.

2. Cleaning

The accepted specimen is then submitted to a thorough cleaning procedure:

1) Wash in Alconox solution and rinse with tap water,
2) Boil in tap water,
3) Rinse
4) Degrease in acetone in ultrasonic cleaner,
5) Dry with nitrogen gas, and
6) Wipe with alcohol.

Disks that are not used immediately are stored in plastic bags with pellets of drierite or silica-gel. (If a relatively long period of storage can be anticipated, the clean disks are stored in a special vacuum desiccator.) In addition, disks made of 1020 steel are sprayed with a rust preventing solution, which is removed just prior to the test by repeating steps 4 through 6. After the test, the rust preventing solution is applied again. It is, therefore, necessary to clean steel disks thoroughly before examination or measurement of surface conditions.

C. Vacuum History of Tests

1. Outgassing of Powders and Baking of System

The measured outgassing rates for basalt and quartz stored in glass jars under normal ambient conditions were very high for these materials (see Appendix B). In order to avoid lengthy pump-downs and adverse effects of desorbing water vapors on ion pumps, the powders used in the vacuum tests were outgassed in a special desiccator prior to their transfer to the experimental chamber. It was found that this procedure reduced pump-down time considerably. Furthermore, the nearly constant gas loads produced by the processed specimens made the achievement of a certain uniformity of the vacuum history of each test easier. Therefore, differences that still exist are due to factors other than the outgassing rates of the mineral specimens. Examples of such factors are exposure time of the whole system to the atmosphere by contamination of vacuum pumps, small leaks — to name two.

Normally, the system is roughed down to 10^{-6} torr within 90 to 120 minutes, when baking is started. Temperatures are increased gradually until maxima are reached; these vary from section to section, and their limitations are set by high temperature sensitive components in the system; e.g., strain gauges and ion pump magnets. Increments of temperature increase are determined by the pressure evolution of the system, which is never allowed to exceed 5×10^{-5} torr. During the entire baking cycle, a temperature gradient ranging from 350 to 400°C at the cryopump to 180 to 200°C at the ion and titanium sublimation pump is maintained. The chamber itself is usually kept at 200 to 210°C. Total baking times have been as low as 24 hours, in some tests as high as 60 hours. When the system pressure indicates a falling tendency and reaches the low 10^{-7} torr level, the heating system is shut off. From this point it requires approximately 12 to 20 hours to produce an ultimate pressure beyond which further decreases cannot be expected within reasonable periods of time. Although the achieved ultimate pressures have varied from test to test (see Tables 1 and 2), they are, with one exception, all in the 10^{-10} torr range, or lower.

2. Residual Gases and Pressure Evolution During Tests

Gases entrapped in and evolved from rocks are in addition to H_2O which represents the largest volume, primarily CO_2, HCl, Cl_2, H_2, H_2S, CO, CH_4, N_2, and O_2. In basalt specifically, CO_2 is generally near 50 percent of the total gas other than H_2O. Two typical mass scans made with a Veeco Model GA-4 gas analyzer during one of the tests to determine the composition of the residual gases in the system are shown in Figs. 9 and 10. One of the scans was made before baking, and one after baking of the system, the mineral specimen being coarse basalt. The difference in relative peak heights of parent gases and their cracking products before and after baking are indicative of the effectiveness of the baking procedures.

Moving components and sliding surfaces always cause an instantaneous transient increase in the pressure of an ultrahigh vacuum system at the start of motion. As soon as motion ceases, the pressure decreases almost as rapidly to the original pressure level. Such pressure changes have been recorded during all of the vacuum tests, and two examples presented in Figs. 11 and 12 show the range of pressure variations. If one considers the type of materials involved, highly gaseous mineral powders and

Table 1

COEFFICIENTS OF FRICTION BETWEEN ROTATING METAL DISK AND MINERAL POWDER

Test No.	Atmosphere	Pressure (Torr)	Powder and Particle Size (in microns)	Disk			Coefficient of Friction	
				Material	Finish (μ-inch)			
					Before Test	After Test	μ_1	μ_c
1	air		quartz, 250-500	aluminum 7075	2-3	3-4	.29	.26
2	vacuum	7.2×10^{-10}	" "	" "	2-4	3-4	.64	.32
3	air		" "	" "	4	5-6	.30	.26
4	vacuum	2×10^{-9}	" "	" "	3	5-6	.58	.24
5	air		" "	steel 1020	3	4-5	.33	.21
6	vacuum	4.5×10^{-10}	" "	" "	3	4	.42	.25
7	air		" "	" "	2	3	.27	.24
8	vacuum	6×10^{-10}	" "	" "	2-5	3-5	.45	.30
9	vacuum	5.5×10^{-10}	basalt, 250-500	aluminum 7075	4	5-10	.40	.26
10	air		" "	" "	4	5-12	.35	.28
11	air		" "	" "	2-3	2-5	.32	.19
12	vacuum	1.3×10^{-10}	" "	" "	4	5-20	1.20	.23
13	air		" "	steel 1020	3	3-4	.29	.18
14	vacuum	2.5×10^{-10}	" "	" "	2-3	2-5	.35	.25
15	air		" "	" "	2-3	2-4	.26	.22
16	vacuum	3×10^{-10}	" "	" "	2-3	2-4	.63	.28
17	air		basalt, 38-62	aluminum 7075	2-3	2-4	.17	.17
18	vacuum	1.6×10^{-10}	" "	" "	2-3	2-4	.36	.24
19	vacuum	1.1×10^{-10}	" "	" "	3-4	3-5	.52	.25
20	air		" "	" "	3-4	3-5	.35	.22
21	air		" "	steel 1020	3-4	3-4	.25	.19
22	vacuum	2.2×10^{-10}	" "	" "	2	2	.34	.32
23	air		" "	" "	2-3	2-3	.22	.18
24	vacuum	3×10^{-10}	" "	" "	2-3	2-3	.33	.22
25	air		quartz, 38-62	aluminum 7075	2-3	3-4	.27	.27
26	vacuum	1.8×10^{-10}	" "	" "	2-3	3-4	.32	.32
27	air		" "	" "	2-3	3-4	.27	.25
28	vacuum	1.4×10^{-10}	" "	" "	2-3	2-3	.59	.30
29	air		" "	steel 1020	2-3	3-4	.20	.16
30	vacuum	2.8×10^{-10}	" "	" "	2-3	3-5	.32	.32
31	air		" "	" "	3	4	.20	.18
32	vacuum	4×10^{-10}	" "	" "	3	3	.34	.34

Table 2

COEFFICIENTS OF FRICTION BETWEEN ROTATING DISK AND MINERAL POWDER WITH ADDED VARIABLES

Test No.	Atmosphere	Pressure (Torr)	Powder and Particle Size (in microns)	Disk Material	Finish Before	Finish After	Added Variables	Coefficient of Friction μ_i	Coefficient of Friction μ_c
33	vacuum	1.6×10^{-10}	basalt, 250-500	aluminum 7075	3-4	3-6	Long vacuum exposure: 240 hours below 1×10^{-9} torr. Dwelling time of disk on powder: 48 hours	.51	.28
34	air		" "	" "	2-3	3-4		.22	.16
35	vacuum	2.7×10^{-10}	quartz, 250-500	aluminum 7075	2-3	3-5	Long vacuum exposure: 240 hours below 1×10^{-9} torr. Dwelling time of disk on powder: 42 hours	.64	.30
36	air		" "	" "	3-4	3-4		.24	.23
37	vacuum	3.1×10^{-10}	basalt, 250-500	aluminum 7075	3-4	5-7	Change of load to 32 ounces. Long vacuum exposure: 170 hours below 5×10^{-9} torr.	.75	.21
38	air		" "	" "	2-3	8-10		.23	.23
39	vacuum	8×10^{-11}	basalt, 250-500	steel 1020	2-3	3-5	Rotational speed of disk: 25 rpm.	.35	.21
40	air		" "	" "	2	3	" " " " "	.27	.19

relatively large metal surfaces in rotational contact, the magnitude of the pressure transients must be considered minimal, thereby indicating the effectiveness of the baking procedures and the presence of a clean system.

3. Effect of Pumping on Powder Samples

In spite of the great care that was exercised when opening and closing valves at the beginning of pump-downs and when bringing the system back to atmospheric pressures at the end of a test, the arrangement of the test powders were disturbed. Sometimes visual inspection through the large viewing port in front of the chamber revealed small crater-like deformations of the surface of the powder sample. Sometimes particles were found on the bottom of the chamber as a result of in-rushing or out-rushing gases. Fluctuations of the pressure during tests also indicate the existence of pressure gradients within the powder beds, and these gradients may affect the measured values of the coefficient of friction. Variations in the appearance of the powder samples after tests are discussed below.

D. Performance of Test

1. General Procedure

Once an acceptable pressure level has been obtained, the following procedure is used to measure the coefficient of friction.

1) The calibration of the strain gauge amplifier and recorder is checked.
2) The speed of the rotating disk is checked.
3) The loaded, stationary disk is then lowered until the disk comes to rest on the powder. It is left in this position for 5 minutes.
4) Next, rotation of the drive in the clockwise direction is started, and stopped after one minute.
5) The direction of rotation is reversed and maintained for one minute.
6) Disk is raised.
7) The calibration of the strain gauge instrumentation is rechecked.

2. Load and Rotational Speed

In the present series of tests, the applied load is 2.5 lbs except for test #37. This value had been chosen to result in a pressure of 1.4 psi, which is equal to the pressure applied during previous phases of the program. The rotational speed was 3 rpm in all but one test, which was performed at 25 rpm for the purpose of investigating the effect of speed of rotation on the coefficient of friction. The reported coefficients of friction are based on measurements made during clockwise rotation.

3. Inspection of Specimens

At the completion of a test, the surface of the disk was examined, its finish measured again, and the changes noted. After some of the vacuum tests, strong adhesion of mineral powders on the contact surface and the rim of the disk were observed (see Fig. 13). The shape of the powder bed in the sample cup at the end of the test showed variations from test to test. Two typical cases are illustrated in Figs. 14 and 15. No dependence on particle size or material has been noted. However, the case illustrated in Fig. 14 is more typical of the condition of the powder bed after vacuum tests, whereas Fig. 15 shows the normal appearance after most air tests. When the vacuum test resulted in the type of powder bed shape shown in Fig. 15, it was sometimes accompanied by strong adhesion among the powder particles throughout the whole bed.

IV. EVALUATION OF RECORDS

A. Processing of Raw Data

As indicated in the description of the torque measuring strain gauge system, it was impractical to compensate completely for the interaction of the strain gauges at the low level of strains measured. This interaction was due to an unavoidable, small eccentricity of the load that caused bending in the hollow shaft in which the gauges were mounted. As a result, the records of torque measurements included this interaction effect which amounted to a cyclic error that normally did not exceed ±25% of the measured torque. Also, in some instances the interaction of high frequency vibrations from nontraceable extraneous sources were superimposed on the records.

In order to exclude the errors introduced by the interaction of gauges and extraneous sources, the raw data were processed in the following manner. When visual inspection of the records indicated that the cyclic error was insignificant, the average value of the readings during the first revolution, exclusive of initial values, was determined and accepted in the calculation of the coefficient of friction. When the cyclic error was deemed significant, a cycle was selected, as close to the start of the test as possible, which clearly showed the variation due to the interaction of gauges. This cycle included the readings between two points where the error due to the interaction of gauges was extreme and of the same sign, i.e., the cycle extended from one minimum (or maximum) to the next one. The duration of the cycle corresponded to the period of one revolution of the disk, 20 seconds. Slight deviations from this period occurred because no elaborate control of the speed of rotation, in excess of a simple rheostat, was deemed necessary.

The cycle selected by visual inspection was then read at every 1/5 second interval on a semiautomatic Benson-Lehmer LARR-V (Large Area Reader-Recorder), whose analog output was converted into digital counts in the Benson-Lehmer Telepak. The digital data were automatically punched on IBM data cards that are compatible for the IBM 360 computer entry. Computer programs, based on the least squares method and available at Grumman Data Reduction Center, were used to obtain best fitting first and third order curves. The digitalized data as well as the best fit curves were then plotted in a greatly magnified scale using a CALCOMP plotter. Examples of the CALCOMP plots are given in Figs. 16 and 17, which show the results of Tests No. 3 and 7.

The first order fits served the purpose of establishing the best fitting straight line variation of the torque during a cycle. The third order fit was intended to follow the actual record closely and eliminate the errors from sources other than the interaction of the gauges. This would have allowed the separation of the interaction error from the other errors and would establish a correction factor for the interaction error as a function of time (rotation). However, examination of the third order best fitting curves showed that this was possible only in a few instances because the third order fit was not reflecting the changes in the curvature of the trace at the minima or maxima, which were selected as the end points of the cycle.

Examination of the records and first degree fits showed that in the majority of cases there was a slight decrease in the average value of torque represented by the best fitting straight line during the cycle, and in some instances there was a slight increase. In order to clarify whether these changes in torque can be attributed to the change in the friction coefficient or other factors, and to investigate the potentiality of applying this method to the determination of slip-friction relationships, Grumman-supported research was initiated. The results of the preliminary tests and theoretical analyses, to be reported in a Grumman Research Department memorandum, (Ref. 1) indicate that the changes in torque during continued rotation are most likely the result of a redistribution of the stresses beneath the rotating disk. For this reason it was decided to consider that value of the torque that is representative of the friction which was theoretically not affected by any redistribution of the stresses. This value was obtained by extrapolating the best fitting straight line to the zero time. The coefficient of friction pertaining to this torque and computed on the basis of uniform stress distribution was designated as μ_c.

In most of the tests, an initially higher value of friction μ_i was observed than the value pertaining to continued motion (Figs. 18 and 19). This initial value was only slightly higher than μ_c for the tests performed in air, and in most instances significantly higher than μ_c for the tests performed in ultra-high vacuum. In the evaluation of the maximum value of the initial friction, consideration was given to its relative position to the cyclic interaction error, and adjustments were made where necessary.

B. Computation of the Coefficient of Friction

As a result of the data processing described in the previous section, torque values representative of the initial condition and continued rotation were established. The coefficient of friction was computed from the above torque values by the formula

$$\mu = \frac{3T}{2WR} \quad ,$$

where

μ = coefficient of friction,

T = torque in inch-ounces,

W = load in ounces, and

R = radius of disk in inches.

This formula is based on the assumption that the distribution of normal and shear stresses beneath the disk is uniform.

Investigations in connection with the Grumman-supported research, referred to earlier, showed that departures from the uniform pressure distribution are possible. The magnitude of these departures, however, is dependent on the actual disk and container dimensions, the applied load, and the ratio of the metal-soil friction to the internal friction of the soil. Parallel tests with annular disks are necessary in each specific case to establish both the effect of nonuniform stress distribution on the torque and an adjustment factor that may be applied to the formula. Preliminary tests made with annular disks of about 1.6 in. O.D. and 0.8 in. I.D. indicate that the effect of departures from the uniform stress distribution on the torque is probably minor in the case of the 1-1/2 in. diameter disk.

V. EVALUATION OF TEST RESULTS

General

The purpose of the testing program was to evaluate the effect of ultrahigh vacuum on the coefficient of friction between metals and soils. However, the testing program was limited to the determination of the rotational sliding resistance under a given normal load. Consequently, for the determination of the coefficient of friction, it had to be assumed that the sliding resistance is composed entirely of friction and adhesion is zero. This assumption is reasonable for dry granular soils tested under atmospheric conditions, but is not justified when adhesion between metal and soil develops in ultrahigh vacuum. Differentiation between friction and adhesion would have required the performance of several tests for each combination of metal and soil by varying the normal load only.

In order to make a quantitative comparison between the frictional resistance in ultrahigh vacuum and air, a coefficient of friction was computed for every test on the assumption that the sliding resistance is entirely frictional. It is emphasized, however, that the computation of a friction coefficient does not denote that the sliding resistance is entirely frictional.

A sample of the records indicating the frictional resistance at various stages of rotation is that shown in Figs. 18 and 19. The recording shows a sharp peak at the beginning of rotation; this peak value is termed the "initial friction," and the coefficient of friction calculated from the peak resistance is designated as μ_i. Sometimes the initial peak is missing and the development of the friction is gradual as indicated by the curve of Fig. 20. In either case, after a comparatively small amount of rotation, the frictional resistance tends to assume a constant value, although various factors, discussed later in more detail, may tend to decrease or increase the observed frictional resistance as the rotation continues. This constant frictional resistance is termed kinetic friction, and the coefficient of friction calculated from the observed frictional resistance is designated as μ_c. Final results, including a detailed description of individual test conditions, are summarized in Tables 1 and 2.

The effect of high vacuum on the initial and kinetic friction is evaluated in the following paragraphs in detail.

Initial Friction

The testing program provided for two tests on each of the eight combinations of two types of metals, two types of materials, and two particle sizes. The initial friction observed in the vacuum tests was generally much higher than either the initial friction observed in air on a comparable combination or the kinetic friction observed in vacuum. In some instances, as for example in the case of steel sliding on fine basalt, the initial friction showed wide variation in the two similar tests. These cases were investigated in detail to find the cause of the discrepancy; two of the additional tests (Nos. 33 and 35) were conducted for the purpose of investigating whether the vacuum exposure time which varied to some extent in the tests, had any effect on the initial friction. As the long exposure tests (Nos. 33 and 35) indicate, the initial friction did not increase in any significant degree when the vacuum exposure was prolonged for a period of over 240 hours. However, a detailed examination of the full vacuum history of the tests that showed inconsistent results (Tests No. 22 versus No. 24 and No. 26 versus No. 28) revealed that in those tests that showed inconsistently low initial friction (Nos. 22 and 28) the pump-down was interrupted because of the malfunctioning of some component and restarted again after the necessary repairs were completed. One consequence of the repetition of baking and pumping down might have been that the loosening of the specimen due to differential gas pressures mentioned in Section III was more intense than in the other tests, and thereby resulted in a possibly lower initial friction.

A quantitative measure of the effect of ultrahigh vacuum on the initial friction can be obtained if the initial friction coefficient in UHV (μ_{iv}) is compared to the initial friction coefficient in air μ_{ia} or to the coefficient of kinetic friction in vacuum μ_{cv}. Unfortunately, the tests results do not lend themselves readily for a statistical analysis of the effect of variables, nor for the analysis of the magnitude of empirical errors, because the testing program was limited to two tests for each combination of the variables. However, tentative conclusions concerning the effect of a selected variable may be drawn from the $\mu_{iv}:\mu_{ia}$ and $\mu_{iv}:\mu_{cv}$ ratios, which are tabulated in Tables 3, 4, and 5 in various combinations for the convenience of evaluation.

Table 3

EFFECT OF TYPE OF METAL ON THE INITIAL FRICTION

Disk	Steel 1020		Aluminum 7075	
Granular Material	μ_{iv}/μ_{cv}	average	μ_{iv}/μ_{cv}	average
Coarse quartz	1.68 1.50	1.59	2.00 2.42	2.21
Coarse basalt	1.4 2.24	1.82	1.54 5.22	3.38
Fine quartz	1.0 1.0	1.0	1.0 1.97	1.48
Fine basalt	1.06 1.50	1.28	1.5 2.08	1.79
	μ_{iv}/μ_{ia}	average	μ_{iv}/μ_{ia}	average
Coarse quartz	1.27 1.66	1.46	2.20 1.93	2.06
Coarse basalt	1.20 2.40	1.80	1.14 3.74	2.44
Fine quartz	1.60 1.70	1.65	1.18 2.20	1.69
Fine basalt	1.36 1.50	1.43	2.12 1.48	1.80

Table 4

EFFECT OF TYPE OF SOIL ON THE INITIAL FRICTION

Material		Quartz		Basalt	
Part. Size	Disk:	μ_{iv}/μ_{cv}	average	μ_{iv}/μ_{cv}	average
Coarse	Steel	1.68	1.59	1.4	1.82
"		1.50		2.24	
"	Alum.	2.00	2.21	1.54	3.38
"		2.42		5.22	
Fine	Steel	1.0	1.0	1.06	1.28
"		1.0		1.50	
"	Alum.	1.0	1.48	1.5	1.79
"		1.97		2.08	
		μ_{iv}/μ_{ia}	average	μ_{iv}/μ_{ia}	average
Coarse	Steel	1.27	1.46	1.20	1.80
"		1.66		2.40	
"	Alum.	2.20	2.06	1.14	2.44
"		1.93		3.74	
Fine	Steel	1.60	1.65	1.36	1.43
"		1.70		1.50	
"	Alum.	1.18	1.69	2.12	1.80
"		2.20		1.48	

Table 5

EFFECT OF PARTICLE SIZE ON THE INITIAL FRICTION

Particle Size		Coarse		Fine	
Material	Disk:	μ_{iv}/μ_{cv}	average	μ_{iv}/μ_{cv}	average
Quartz	Steel	1.68 1.50	1.59	1.0 1.0	1.0
"	Alum.	2.00 2.42	2.21	1.0 1.97	1.48
Basalt	Steel	1.4 2.24	1.82	1.06 1.50	1.28
"	Alum.	1.54 5.22	3.38	1.5 2.08	1.79
		μ_{iv}/μ_{ia}	average	μ_{iv}/μ_{ia}	average
Quartz	Steel	1.27 1.66	1.46	1.60 1.70	1.65
"	Alum.	2.20 1.93	2.06	1.18 2.20	1.69
Basalt	Steel	1.20 2.40	1.80	1.36 1.50	1.43
"	Alum.	1.14 3.74	2.44	2.12 1.48	1.80

From the tabulations, the following tentative conclusions can be drawn.

a) The magnitude of the initial friction in ultrahigh vacuum relative to that in air is consistently higher with steel disks than with aluminum disks. (The over-all average ratio is 2.0 in all tests with aluminum compared to 1.58 with steel.)

b) In ultrahigh vacuum, basalt appears to develop a somewhat higher ratio of initial friction to kinetic friction than quartz. The over-all average ratio of initial to kinetic friction is 2.07 for basalt compared to 1.58 for quartz.

c) Particle size does not appear to have significant effect on the initial friction.

This last finding is somewhat contrary to expectation since decreasing particle size should result in relatively stronger bonds between the particle and metal. There are several reasons, however, why in this type of test the effect of decreasing particle size does not manifest itself in an increase of the initial friction. First, the loosening effect of gas bubbles, discussed earlier, comes into play primarily with the finer particles which form a bed with low gas permeability. Second, the measured initial friction between metal and soil cannot exceed the value of soil to soil friction, because in the case of strong adhesion of the particles to the metal, rotation would take place in the soil itself. The soil to soil friction of the finer particles may be appreciably lower than that of the coarser particles. Finally, the fine particles tend to develop some initial friction in air, thereby making the difference in initial friction between tests in air and ultrahigh vacuum smaller.

In the testing program the last four vacuum tests were left open to permit further investigation of the effect of some of the variables observed during the first 16 tests. The purpose of tests Nos. 33 and 35 was to investigate the effect of long vacuum exposure. As may be seen from the comparison of initial friction coefficients with the comparable tests (No. 33 versus Nos. 10 and 13, and No. 35 versus Nos. 3 and 5, see table 2), the difference in initial friction between normal and long vacuum exposure, if any, is within the experimental error.

Test No. 37 was conducted with a lower normal load. The purpose of this test was to investigate the nature of what is termed the "initial friction." If the cause of the observed high sliding resistance is adhesion, it is expected to act with the same value under lower normal load resulting in a higher computed value of

the "initial friction." Test No. 37 was inconclusive in this respect, inasmuch as the computed coefficient of initial friction μ_i was inbetween the values obtained with the comparable tests at higher normal load (0.70 in test No. 37 compared to 0.40 in test No. 9 and 1.2 in test No. 12). Further tests are needed to clarify the nature of the high initial sliding resistance observed in the tests performed in ultrahigh vacuum.

Test No. 39 was conducted for the purpose of investigating the effect of speed on the friction between metals and soils. If rotational speed has any effect on the initial friction, it is less than the experimental error.

Kinetic Friction

In general, the effect of ultrahigh vacuum on the kinetic friction is less pronounced than that on the initial friction, and the differences observed between comparable values of kinetic friction in air and ultrahigh vacuum are often in the range of experimental error. In order to evaluate the effect of ultrahigh vacuum in such cases, a statistical evaluation of the mean of the observed values with respect to the standard deviation would be necessary. In view of the small number of tests (two) performed under comparable conditions for each combination of the variables, a statistical evaluation of the experimental error is not practical. A quantitative measure of the effect of the ultrahigh vacuum is the ratio of the kinetic friction coefficient in vacuum over that in air, $\mu_{cv}:\mu_{ca}$. These ratios, tabulated in various groupings in Table 6, allow a simple comparison of average values, which can serve as a basis for a tentative evaluation of the effect of each variable.

From Table 6, the following tentative conclusions can be drawn. Generally, there is an increase in the coefficient of kinetic friction when the materials are exposed to ultrahigh vacuum. There were, however, a few instances when a lower coefficient of kinetic friction was observed in ultrahigh vacuum than in air. Since the difference between the observed values is less than the experimental error ($\mu_{cv} = 0.24$ versus $\mu_{ca} = 0.26$ in test No. 4 and $\mu_{cv} = 0.26$ versus $\mu_{ca} = 0.28$ in test No. 9), and the results were not duplicated in the parallel tests, the observed lower values are not considered to represent a trend different from that observed in all of the other tests of the testing program. It is also noted here, that the uncontrolled loosening of the sample bed during baking and pump-down might have contributed to a lower coefficient of friction in these tests.

Table 6

EFFECT OF ULTRAHIGH VACUUM ON THE KINETIC FRICTION

Disk		Aluminum		Steel	
Material	Particle Size	μ_{cv}/μ_{ca}	average	μ_{cv}/μ_{ca}	average
Quartz	Coarse	1.23	1.08	1.19	1.22
	"	0.92		1.25	
Basalt	"	0.93	1.06	1.39	1.33
	"	1.21		1.27	
Quartz	Fine	1.18	1.19	2.00	1.94
	"	1.20		1.88	
Basalt	"	1.41	1.28	1.68	1.45
	"	1.14		1.22	

Material		Quartz		Basalt	
Particle Size	Disk	μ_{cv}/μ_{ca}	average	μ_{cv}/μ_{ca}	average
Coarse	Alum.	1.23	1.08	0.93	1.06
"		0.92		1.21	
"	Steel	1.19	1.22	1.39	1.33
"		1.25		1.27	
Fine	Alum.	1.18	1.19	1.41	1.28
"		1.20		1.14	
"	Steel	2.00	1.94	1.68	1.45
"		1.88		1.22	

Table 6 (Cont.)

Particle Size		Coarse		Fine	
Material	Disk	μ_{cv}/μ_{ca}	average	μ_{cv}/μ_{ca}	average
Quartz	Alum.	1.23 0.92	1.08	1.18 1.20	1.19
"	Steel	1.19 1.25	1.22	2.00 1.88	1.94
Basalt	Alum.	0.93 1.21	1.06	1.41 1.14	1.28
"	Steel	1.39 1.27	1.33	1.68 1.22	1.45

The effect of the individual variables on the kinetic coefficient of friction in ultrahigh vacuum is evaluated as follows:

Effect of type of disk. A glance at the first tabulation of Table 6 indicates that the μ_{cv}/μ_{ca} ratio is consistently higher for steel than for aluminum.

Effect of type of granular material. The second tabulation in Table 6 indicates no consistent trend in favor of either material.

Effect of particle size. The third tabulation in Table 6 indicates that the μ_{cv}/μ_{ca} values are consistently higher for the fine material than for the coarse.

From the additional four tests, further information on the kinetic friction could only be obtained from test No. 39. This test conducted at a high rotational speed (25 rpm) did not show any significant effect of the speed of rotation on kinetic friction.

As indicated before, the values of the coefficient of kinetic friction were determined from the torque values observed during the first revolution. This coefficient was found to change during the test encompassing three revolutions. In some cases, changes in the calculated coefficient of friction were observed even during the first revolution. The coefficients of friction indicated in the tabulation are those evaluated on the basis that the first degree fits are valid at the beginning of the rotation, but not after the initial friction becomes kinetic. In most cases, the calculated value of the kinetic friction tended to decrease with rotation; this is attributed to changes in the pressure distribution beneath the disk and the resulting change in the torque arm rather than to a decrease in the friction. In other cases, an increase of the calculated value of the coefficient of friction was observed. This increase is attributed to an increase of the roughness of the metal disk as rotation progressed. Typical of this case are test Nos. 10 and 12, each of which demonstrated an increase in the kinetic friction with continuing rotation; these tests also showed the greatest increase in the roughness of the metal disk (from 4 to 5-13 microinches in test No. 10 and from 4 to 5-20 microinches in test No. 12).

Miscellaneous Observations

In the tests performed with fine materials, sticking of fine particles to the metals was observed. Some of the particles adhered to the metal even after the vacuum was released. Fig. 13 shows a disk with adhering particles after the release of vacuum. The observed sticking of the particles supports the theory of the initial friction being adhesive in nature.

In some of the tests, it was observed that the grains in the container cup adhered so strongly to each other, even after the vacuum was released, that appreciable effort with a metal scoop was required to remove them from the cup. A review of the histories of the tests where such behavior was observed did not reveal any cause for the coherence of the granular material to be higher in these tests than in others.

VI. CONCLUSIONS AND RECOMMENDATIONS

The series of friction experiments conducted in ultrahigh vacuum (at pressures below 2×10^{-9} torr) with various combinations of metals and granular materials show that ultrahigh vacuum affects the frictional resistance between these dissimilar materials in two ways. First, at the beginning of sliding motion, an initial frictional resistance develops that is about 50 to 150% higher than that experienced under normal atmospheric conditions. Second, the coefficient of kinetic friction is about 6 to 97% higher, depending upon the particular combination of metal and granular material, than that observed under atmospheric conditions. In general, even the higher values of kinetic friction obtained in ultrahigh vacuum are low compared to soil-to-soil friction values of materials similar to those tested and metal on soil friction coefficients commonly encountered in foundation construction.

Because of the present program's limitations, no conclusions concerning the cohesive or frictional nature of the initial frictional resistance can be drawn at this time. It is recommended that the nature of the initial frictional resistance be investigated by further experiments in which the vertical load is the main variable. It is also recommended that the rotational displacement necessary to develop the initial frictional resistance be measured. This information is useful for the application of the data to lunar locomotion studies.

During the testing program, only metals with surface finishes in the 3-6 microinch range were used. In any application where a higher coefficient of friction is desired, the obvious way to achieve this would be to use metals with rougher surfaces. Surface roughness is expected to affect the coefficient of friction in relation to the particle size. Any increase in the coefficient of friction is, however, limited by the internal friction of the granular material. It is recommended that the effect of surface roughness on the coefficient of friction be investigated in a new testing program.

As reported in Section II, various improvements in the testing technique were made in the course of the development of the design of the vacuum equipment, friction measuring apparatus, and associated instrumentation. As a result of the experimental observations, the following recommendations are made to improve further the testing technique.

A method should be devised by which changes in the compactness of the granular sample during outgassing would be prevented. Annular disks, instead of full disks, should be used to avoid the effect of changes in pressure distribution during rotation.

The linear measure of the surface roughness as determined by the profilometer for this test series indicates only the maximum depth of the surface asperities without giving information of the frequency of occurence of such asperities within a certain area of the disk. Since the frictional properties are affected by both the depth and the frequency (or density) of the surface asperities, it is desirable to develop a more meaningful method for the measurement of both of these properties.

In the present system strain gauges are placed outside the vacuum chamber thereby resulting in a strain gauge balance where, due to the extremely low stresses, some interaction of the torque gauges with lateral loads is unavoidable. It is recommended that the applicability of strain gauges inside the vacuum chamber be studied with particular attention given to their outgassing characteristics. A strain gauge balance that is less sensitive to lateral loads should be designed and placed inside the vacuum chamber.

VII. REFERENCES

1. Karafiath, L. L., Some Aspects of the Determination of the Coefficient of Friction between Metals and Soils and its Application to Lunar Locomotion Studies, Grumman Research Department Memorandum RM-379, October 1967.

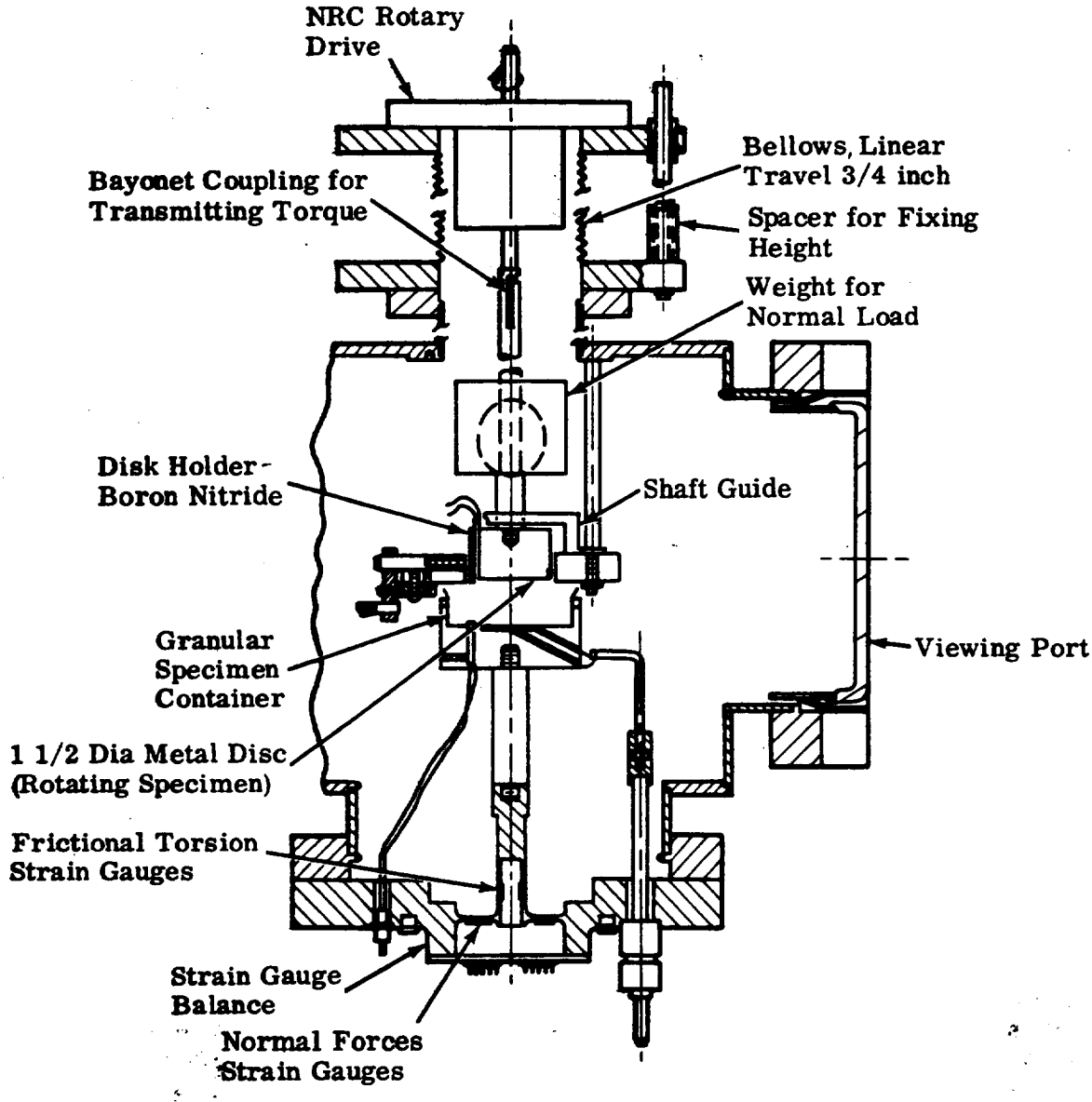

Fig. 1 Friction Measuring Apparatus

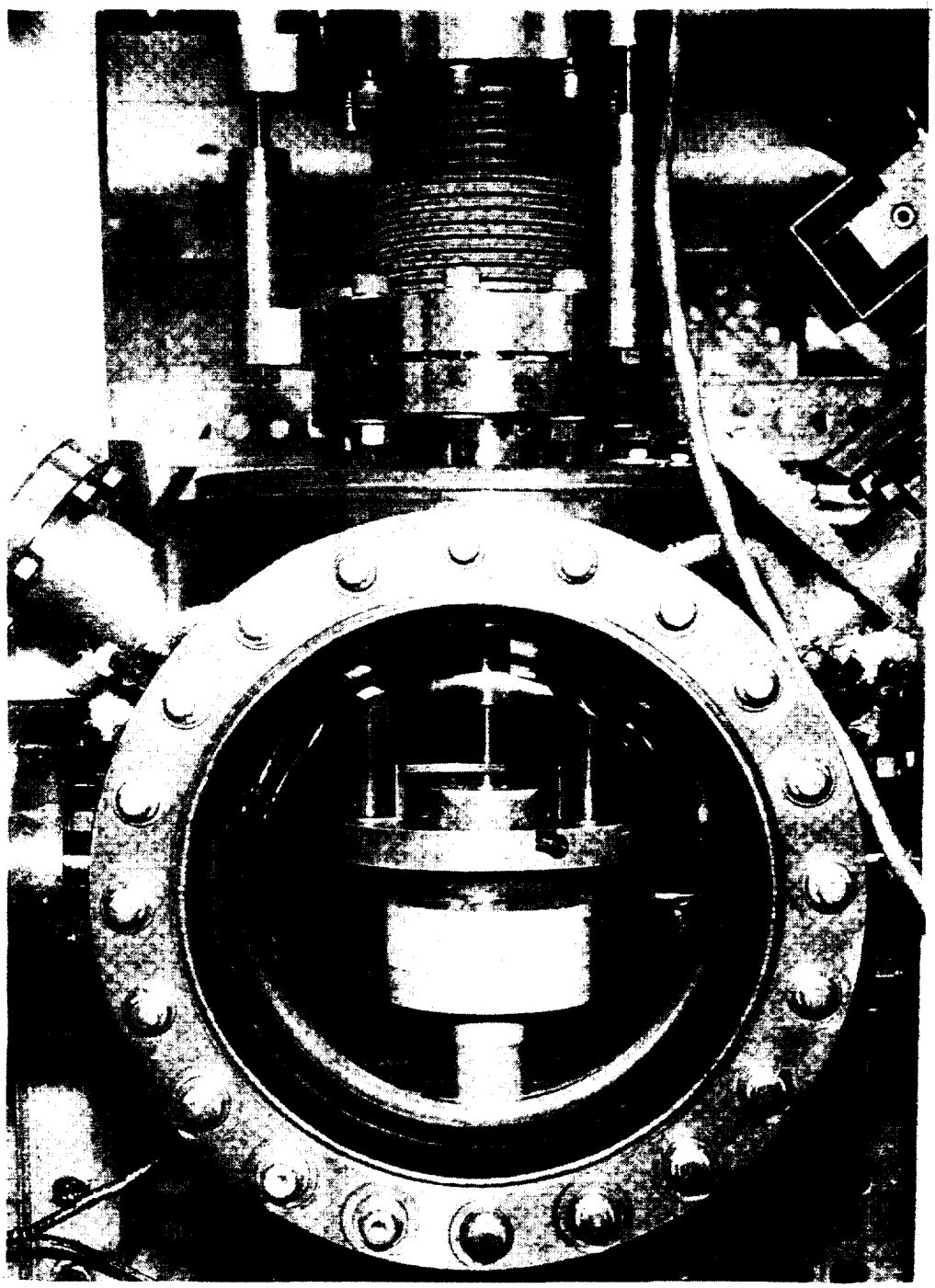

Fig. 2 Position of Metal Disk Holder and Mineral Cup Seen through Viewing Port

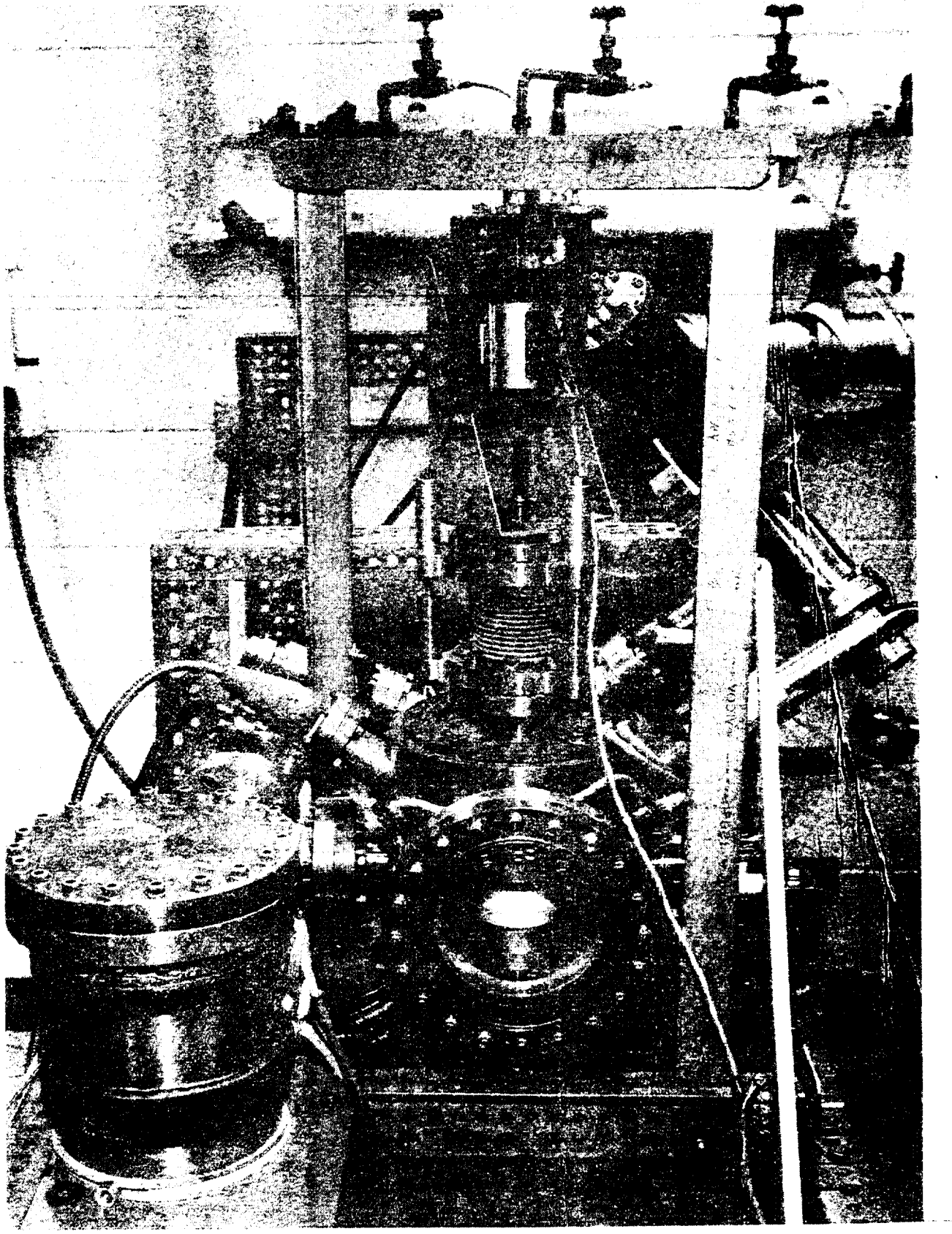

Fig. 3 Vacuum Chamber with External Drive Arrangement for Rotating Disk

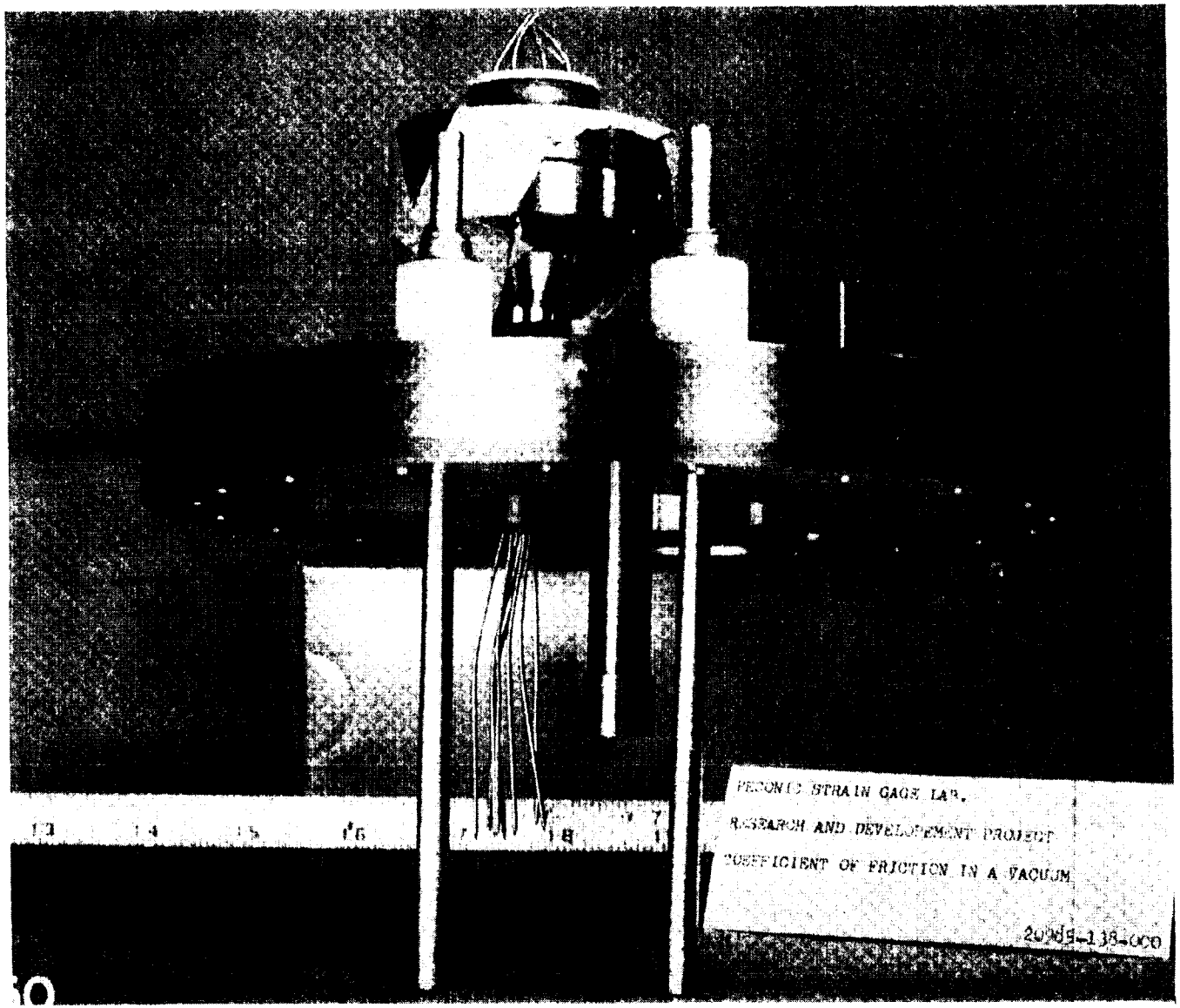

Fig. 4 Strain Gauge Balance, Side View

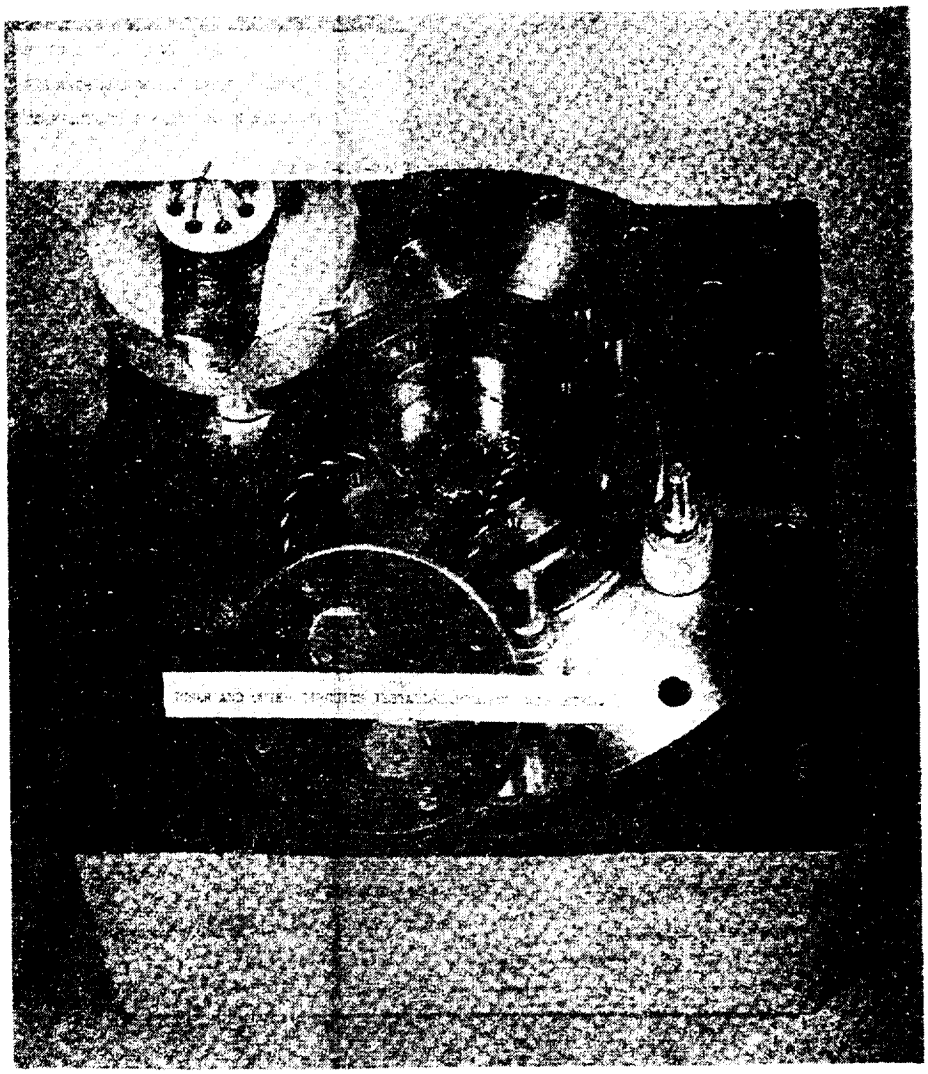

Fig. 5 Strain Gauge Balance, Bottom View

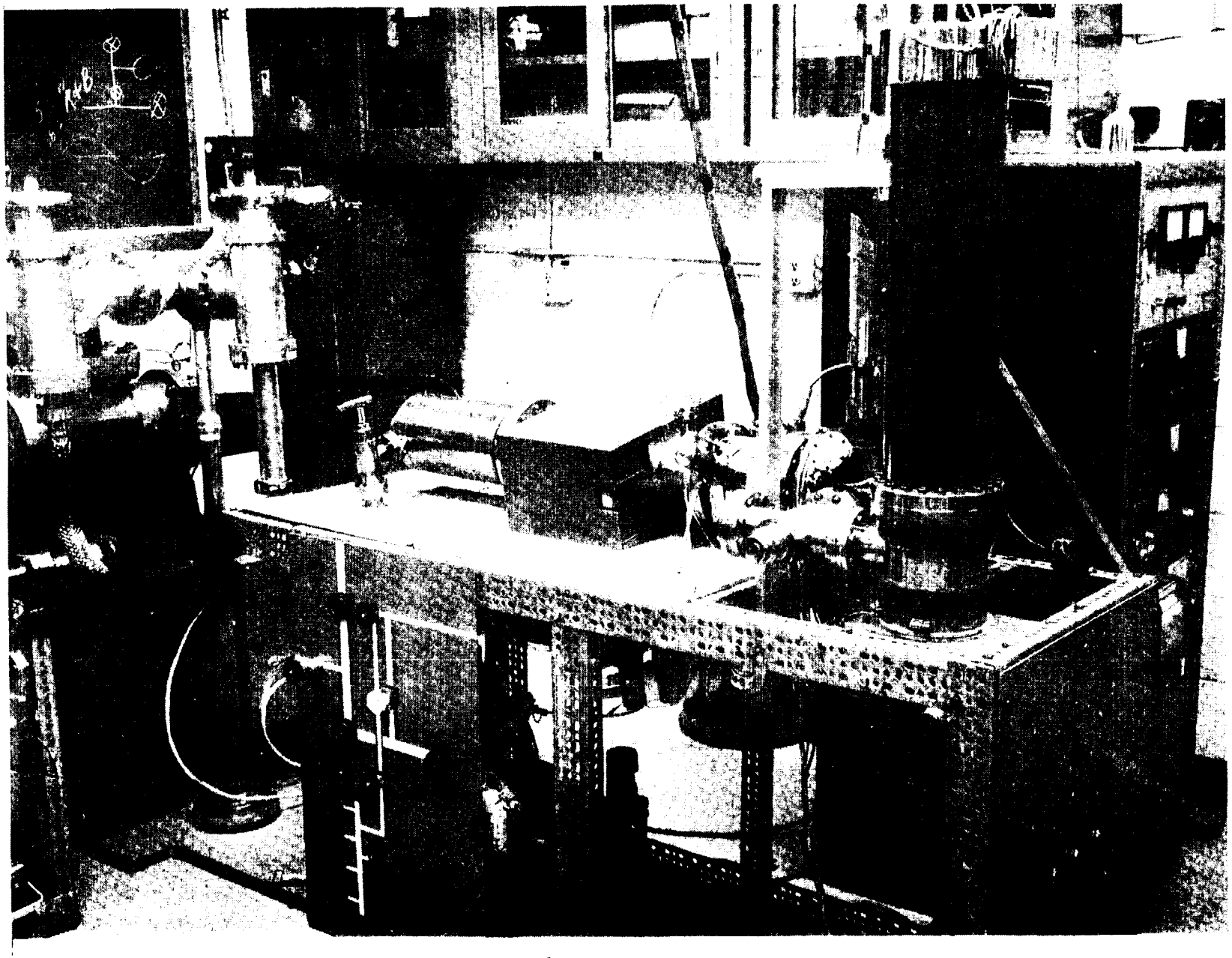

Fig. 6 Ultrahigh Vacuum System

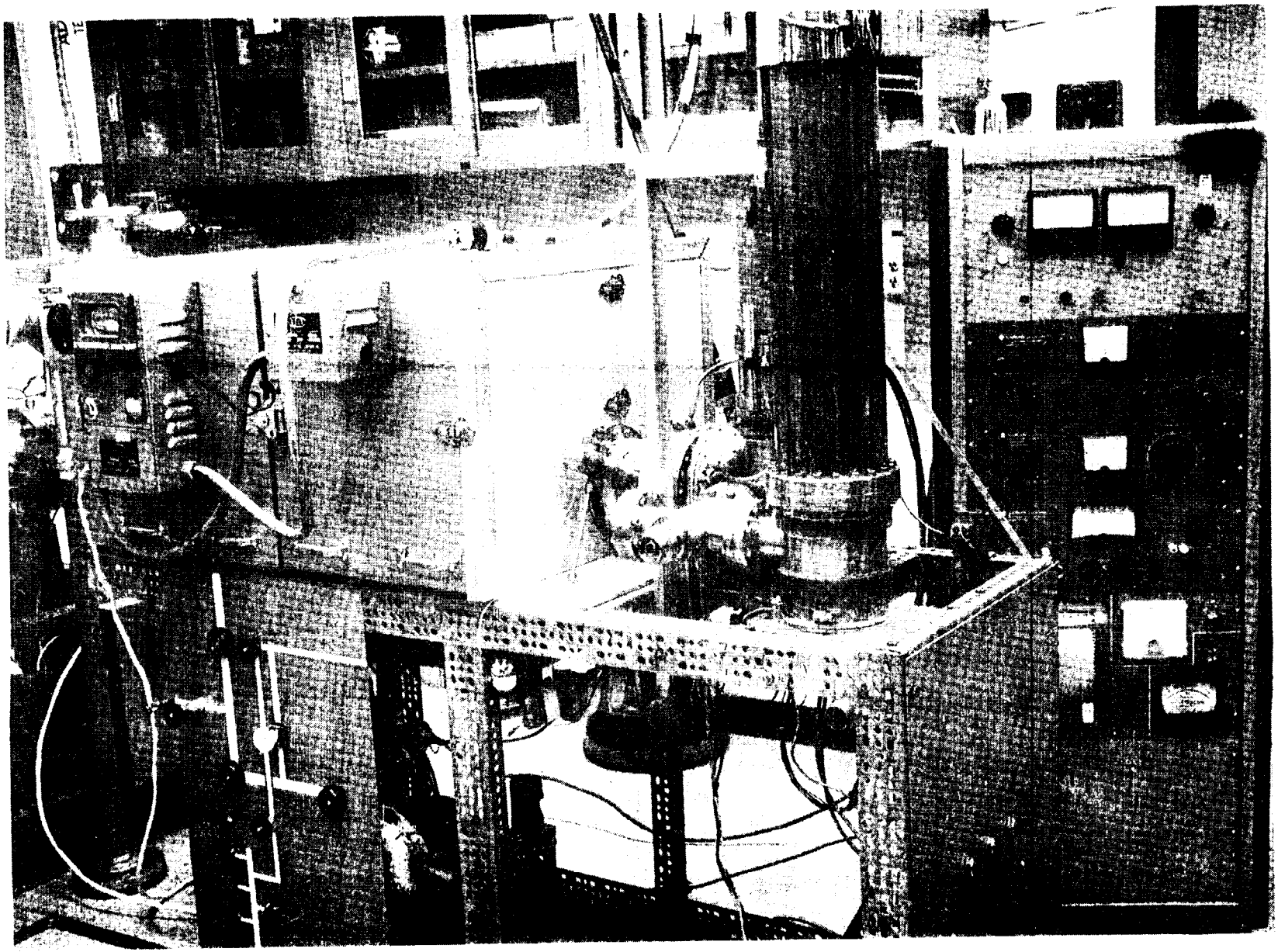

Fig. 7 Ultrahigh Vacuum System with Baking Ovens

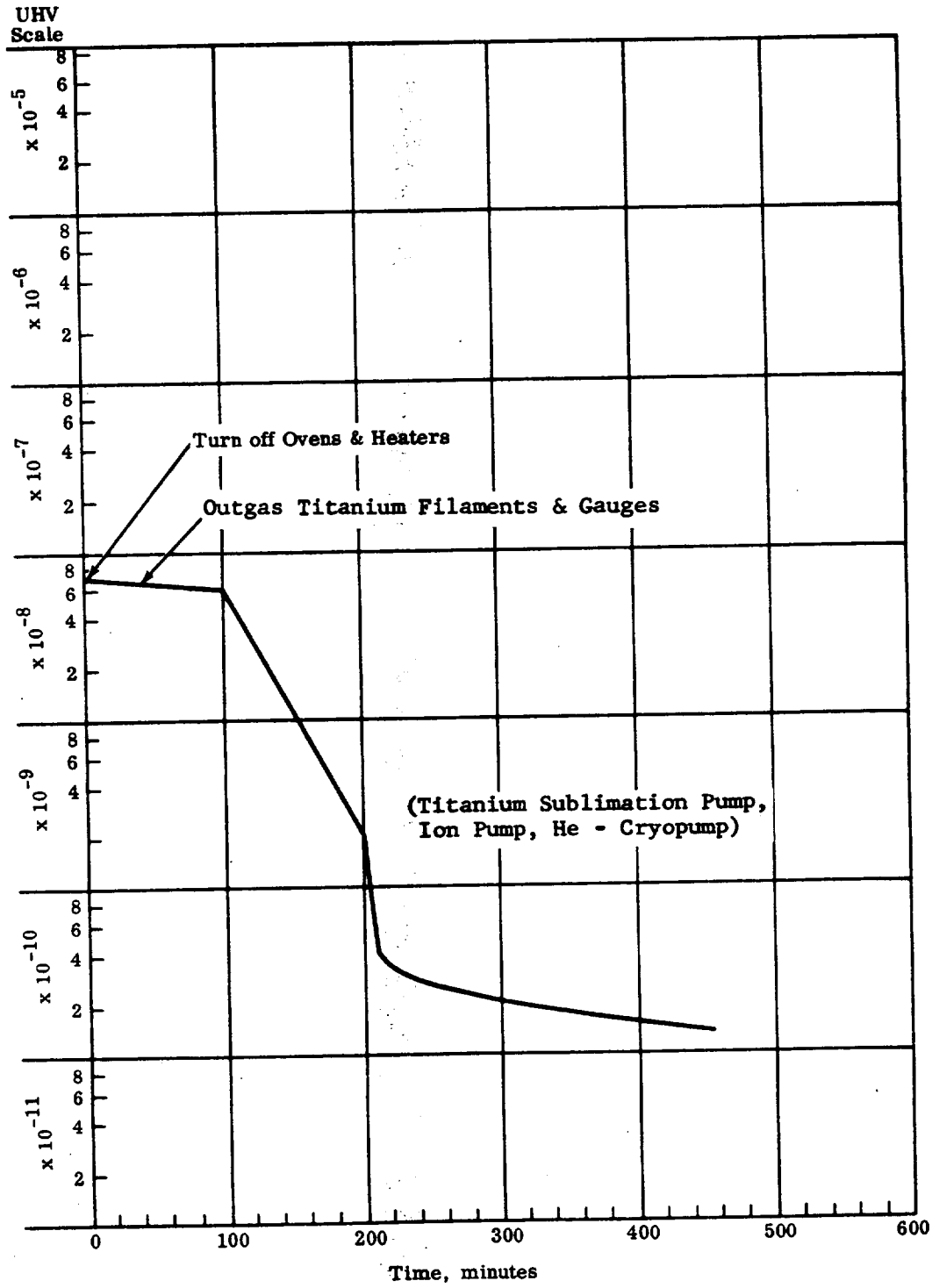

Fig. 8 Pressure Evolution after Baking

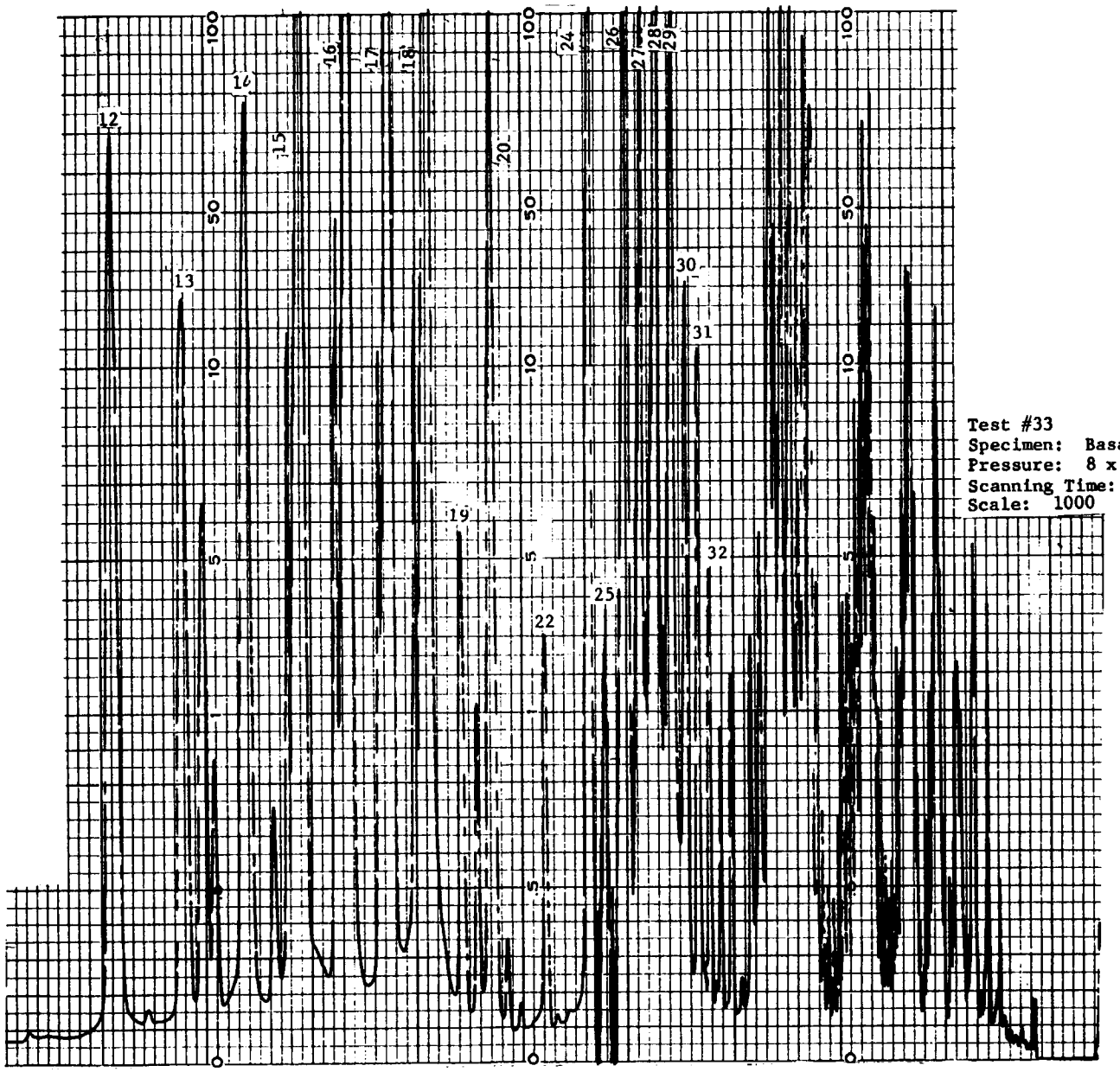

Test #33
Specimen: Basalt, 250-500μ
Pressure: 8×10^{-6} Torr
Scanning Time: 5 minutes
Scale: 1000

Fig. 9 Residual Gases before Baking

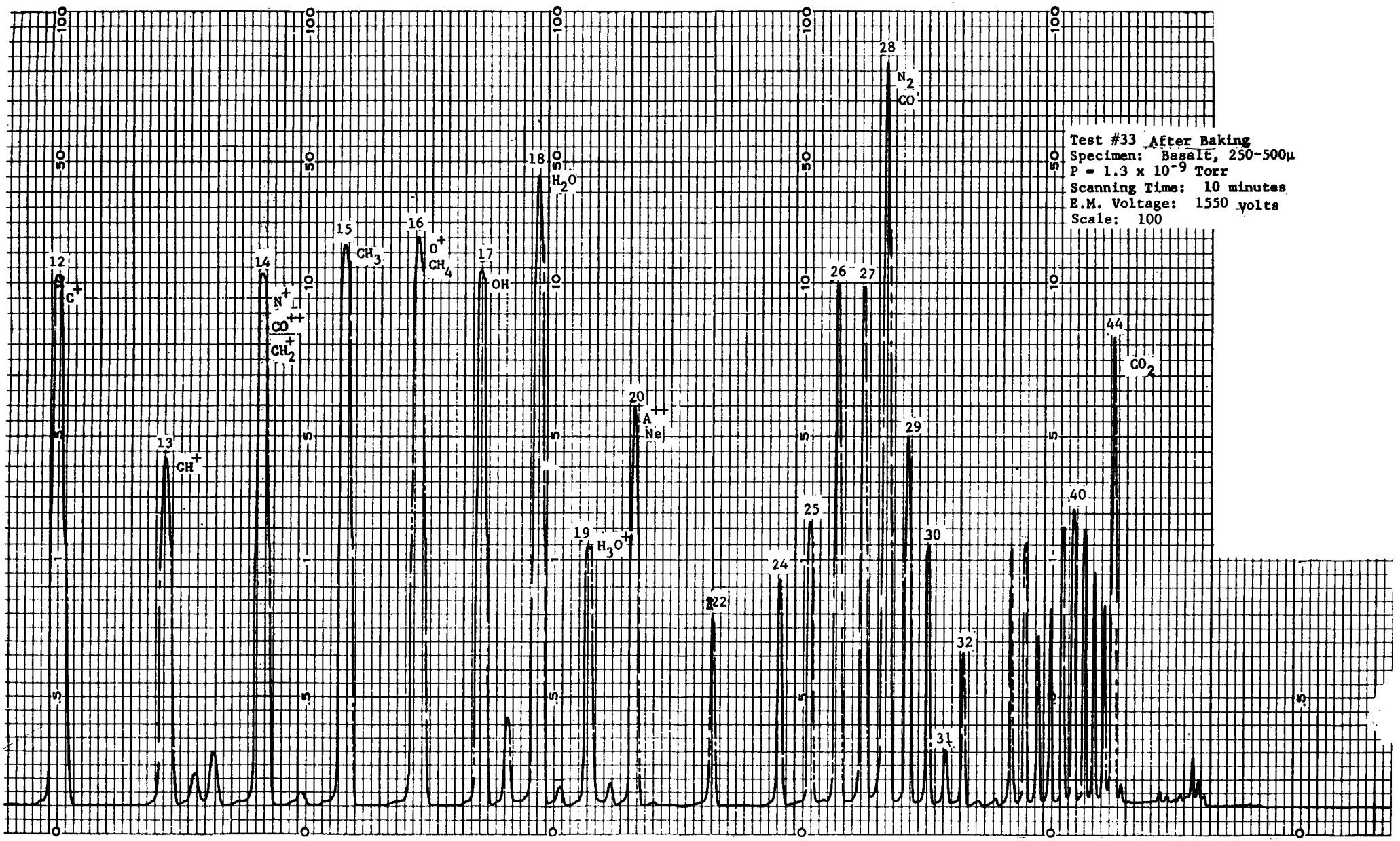

Fig. 10 Residual Gases after Baking

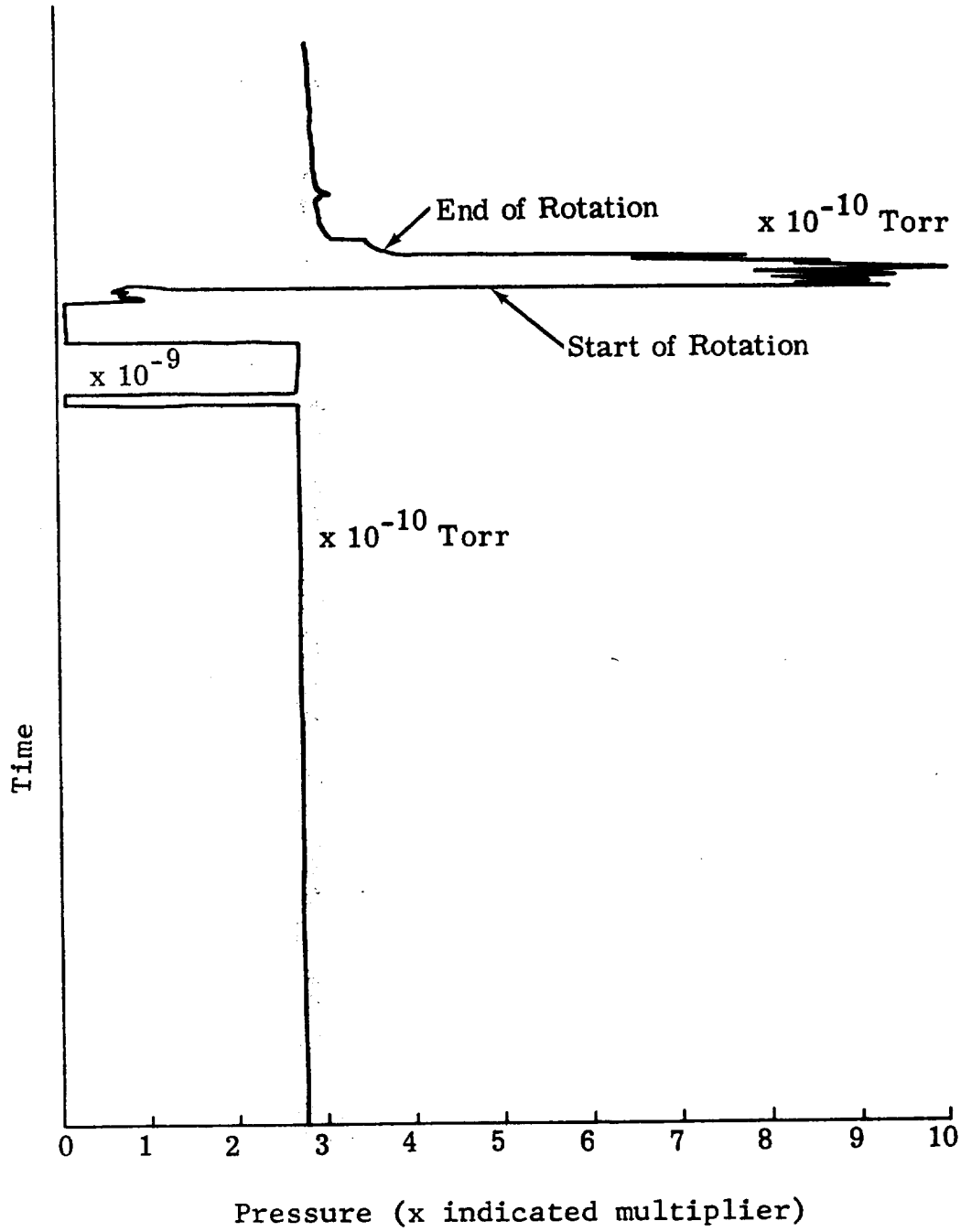

Fig. 11 Recordings of Pressure Evolution During Test #35

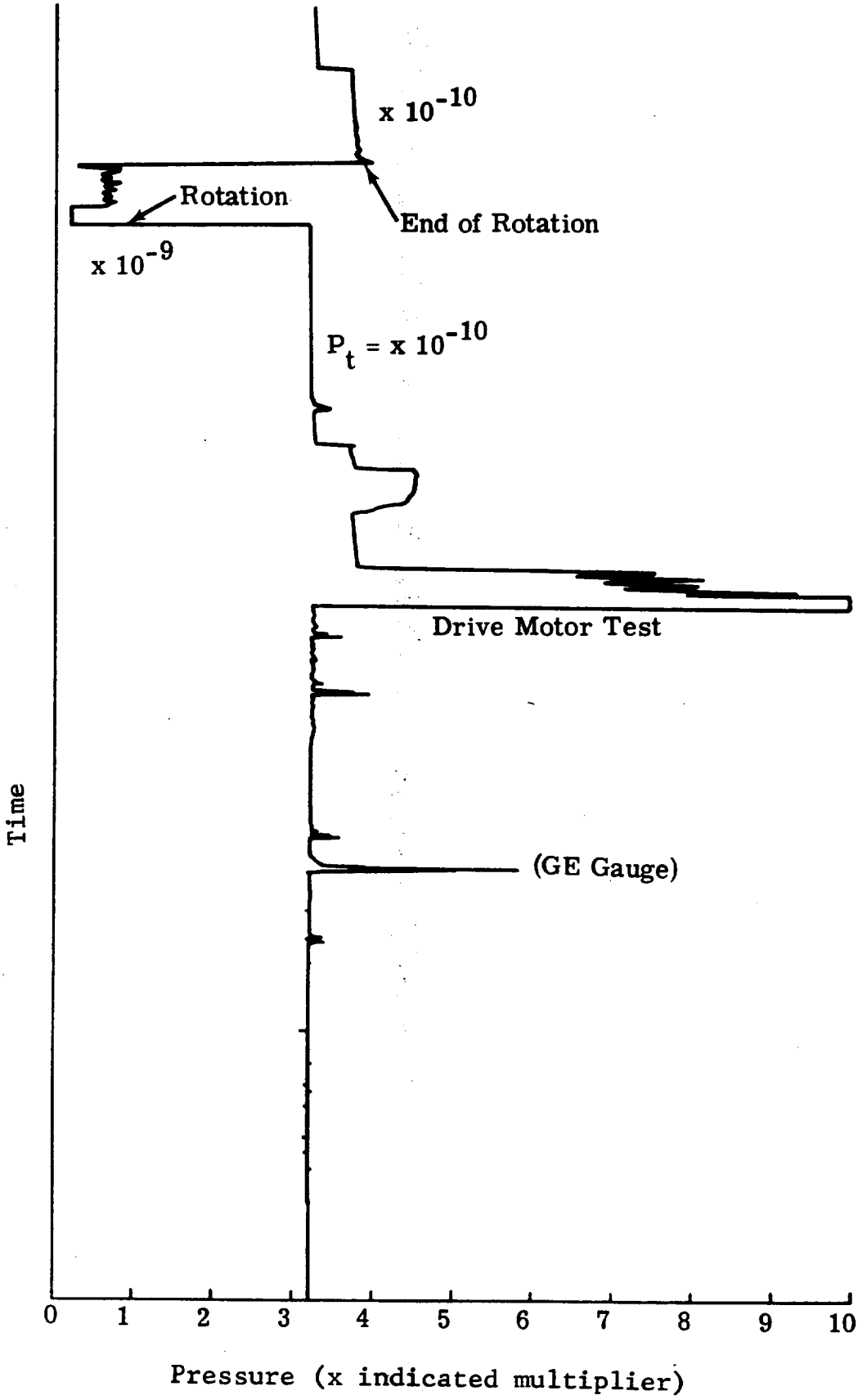

Fig. 12 Recording of Pressure Evolution During Test #37

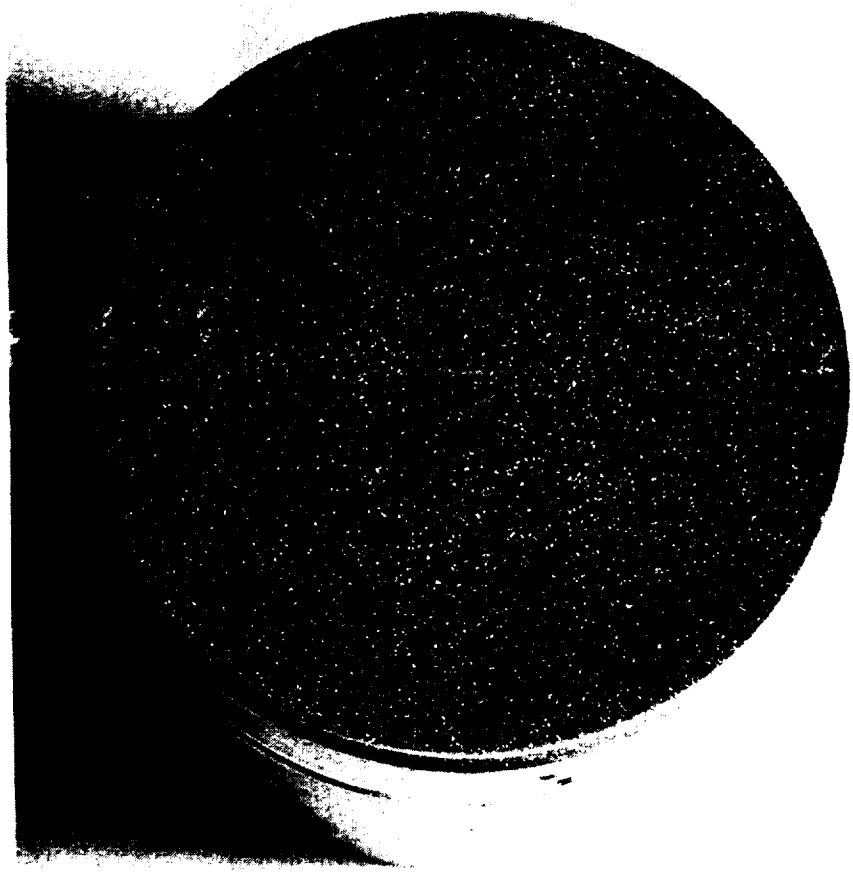

Fig. 13 Adhesion of Mineral Powder on Metal Disk

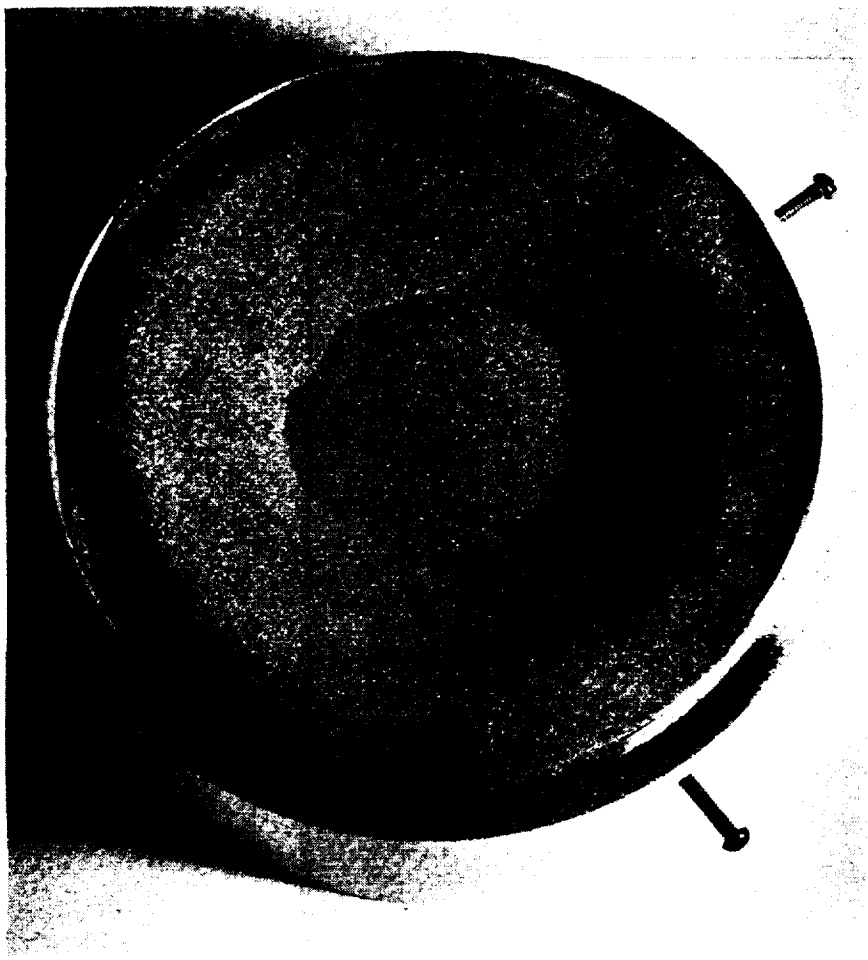

Fig. 14 Appearance of Powder Specimen after Test (Typical of Vacuum Tests)

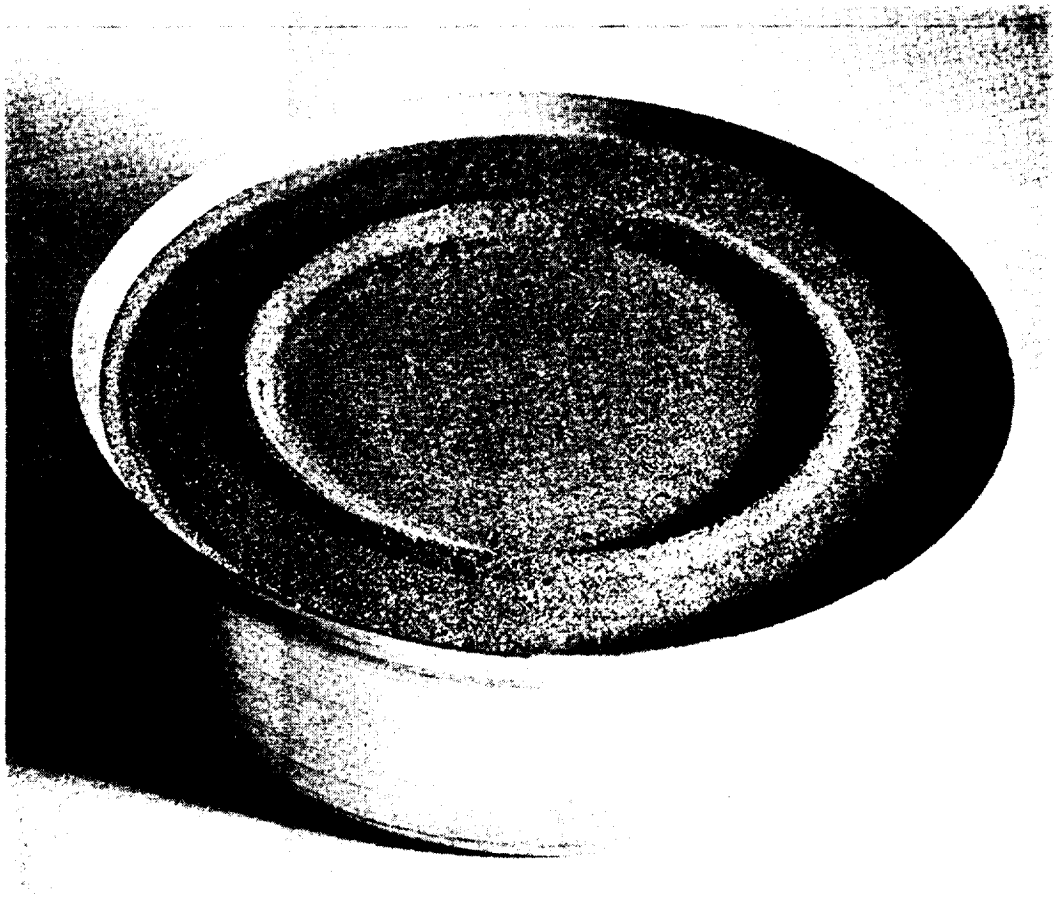

Fig. 15 Appearance of Powder Specimen after Test (Typical of Air Tests)

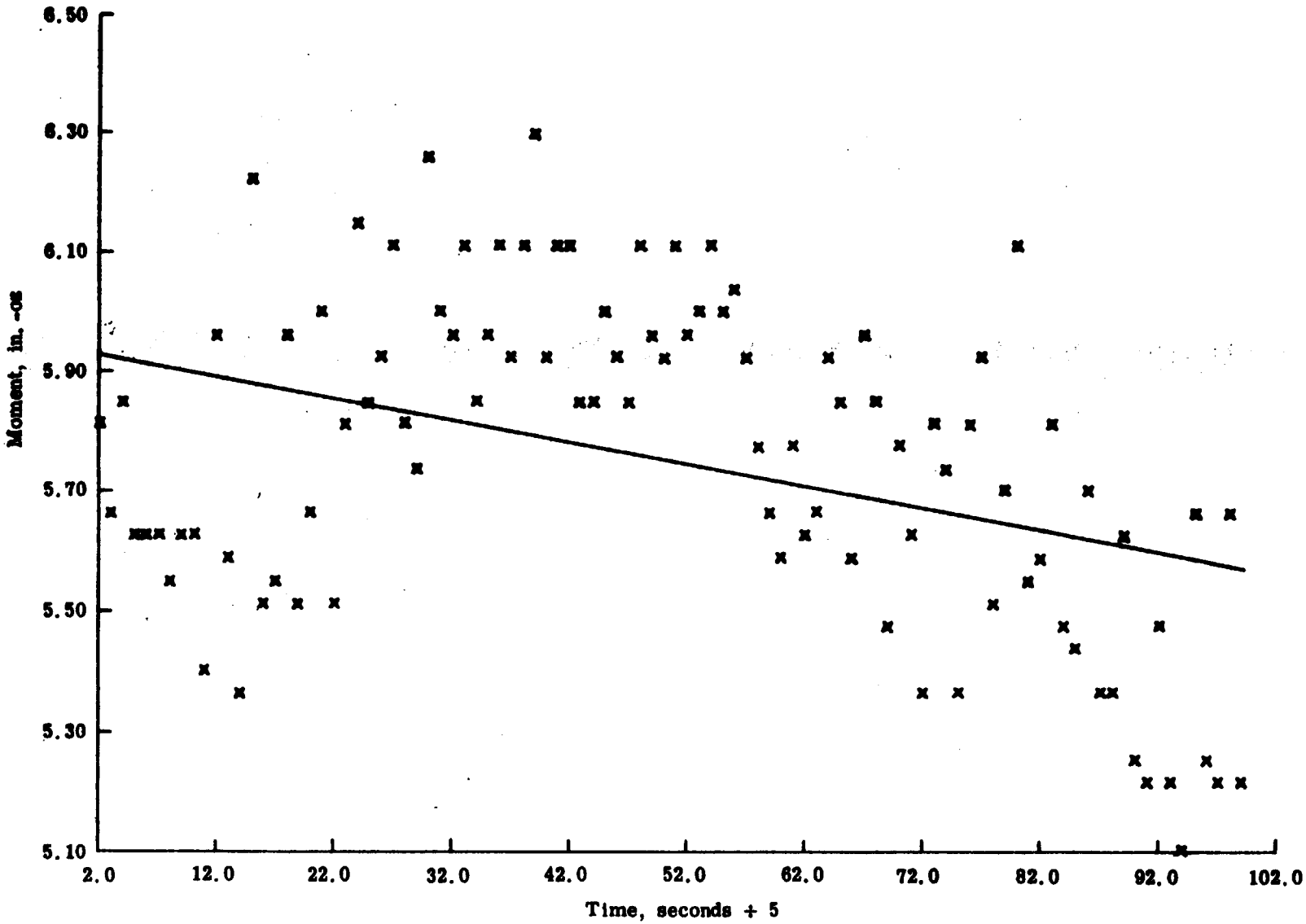

Fig. 16 First Order Curve for Test #3 (best fitting curve by the least squares method)

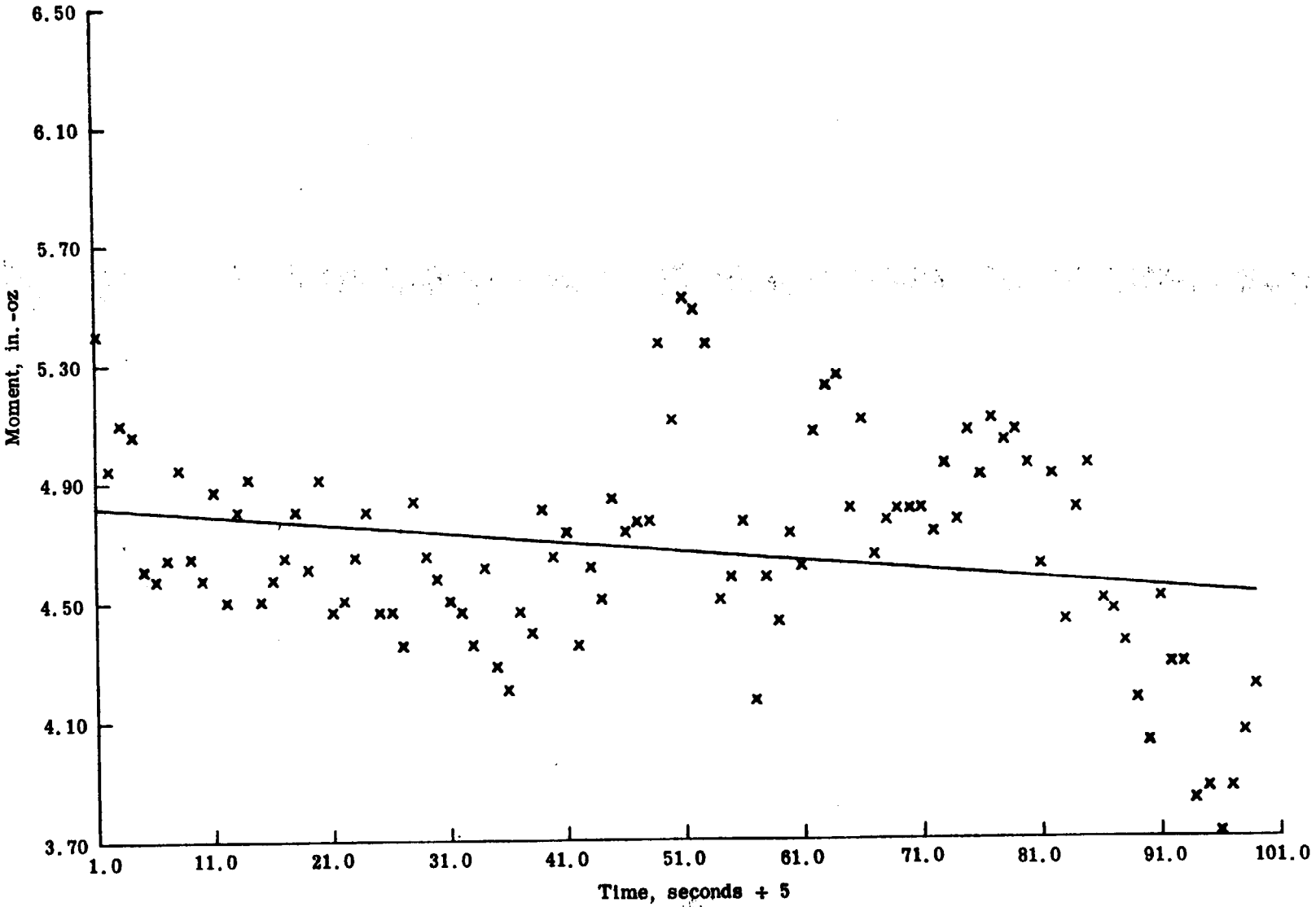

Fig. 17 First Order Curve for Test #7 (best fitting curve by the least squares method)

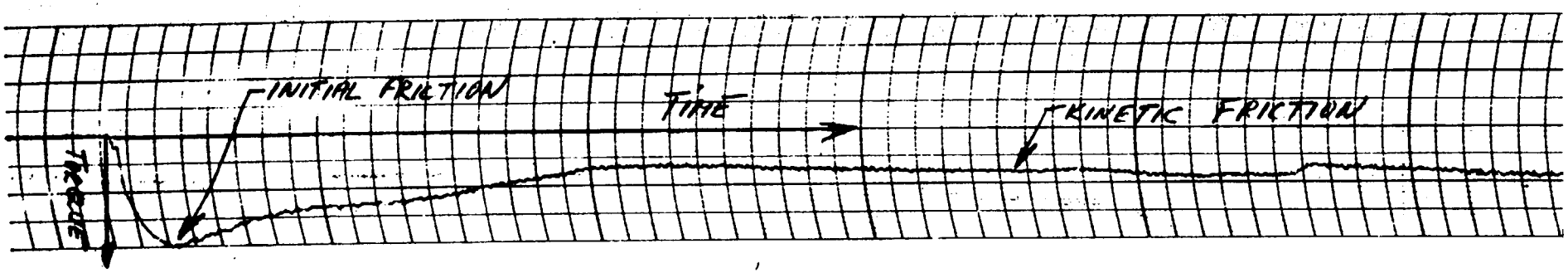

Fig. 18 Recording of Evolution of Friction During Test #28 (Brush Instrument Mark II Recorder)

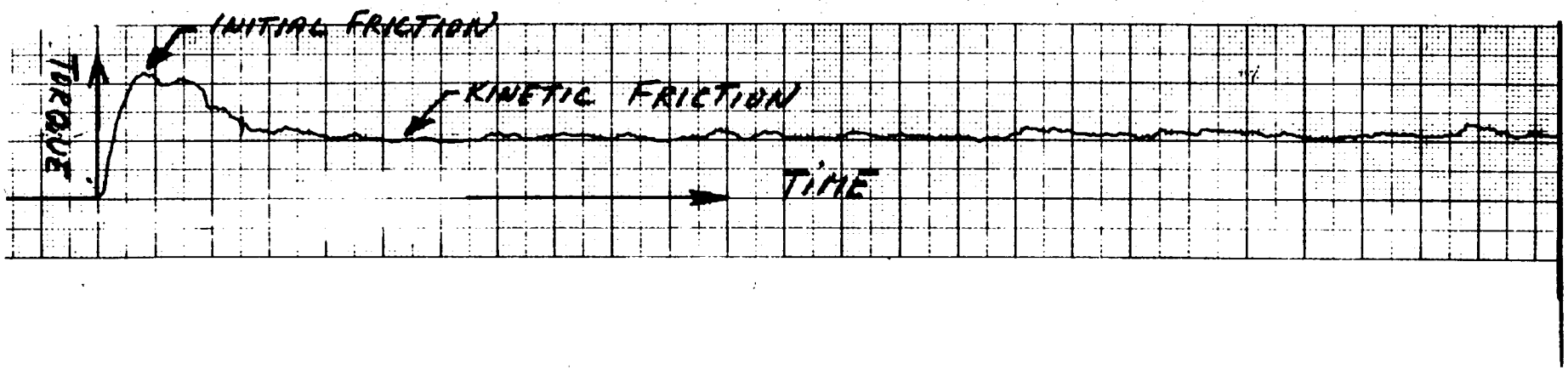

Fig 19 Recording of Evolution of Friction During Test #35
(MASSA-COHU Recording Oscillograph)

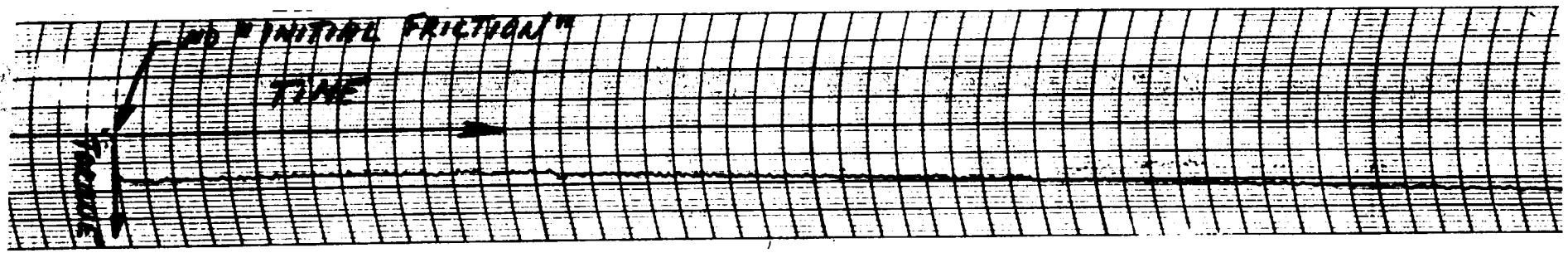

Fig. 20 Recording of Evolution of Friction During Test #25
(Brush Instrument Mark II Recorder)

APPENDIX A

PREPARATION OF GRANULAR MATERIAL

In order to obtain the specified range of particle sizes from the bulk material, various methods of comminuting, sifting, and washing were tried.

Coarse Materials

The procedure adopted for the preparation of coarse granular material (250-500 microns) is as follows:

1. Material, as received, is crushed manually until it passes a No. 8 US-standard sieve.

2. Fine particles, below 105 microns (140 mesh) are eliminated by sieving the crushed material in a motor-driven Ty-Lab tester. The total weight sieved in one operation is approximately 300 grams; the sieving-time is 20 minutes. For several of the sieves containing the finer materials, sieving is continued for an additional 10 minutes. This has proven helpful for removing very fine particles (below 38 microns) from the mixture.

3. The total yield of particles produced between 500 and 250μ is then placed in a 250 mesh sieve and washed with flowing tap water. The sieve is gently agitated until the water flowing through the material and the screen is clear. (Particles below 250μ are stored for ball milling at a later time.)

4. Particles between 8 mesh and 500μ are placed in a ball mill, approximately 900 grams per charge, and milled for 1-1/2 hours. The grinding medium is 1/2-inch diameter tungsten carbide balls.

5. The procedure outlined under steps 2, 3, and 4 is repeated.

A check test on the size distribution of a coarse basalt sample prepared by the above method showed the following results.

SIZE DISTRIBUTION OF COARSE BASALT PARTICLES

(250-500μ)

Sieve Opening (microns)	U.S. Sieve No.	Weight between Sieves (grams) First Run	Second Run	Third Run
500	35			
420	40	29.2	29.9	31.3
350	45	29.1	29.0	29.0
297	50	21.0	20.6	21.3
250	60	25.0	24.7	24.0
210	70	4.9	3.6	3.5
pan		1.0	1.2	0.3
TOTAL		110.2	109.0	109.3

Fine Materials

The preparation of the fine material presented problems inasmuch as comminution by hand-crushing in a stainless steel mortar into coarse particles ranging from 500 to 1700μ and ball milling (tungsten carbide balls) for about two hours yielded very small amounts of the required sizes, as the following tabulation of weights shows.

Weight	Grain Size	% By Weight
g	μ	
42	< 38	4
48	38-62	5
126	62-250	13
220	250-500	22
564	> 500	56
1000		100

Grinding of the larger size particles with stainless steel balls was found to be nearly impossible. Manual wet sieving was attempted, but it turned out to be inefficient and rather messy. The fractionating arrangement, shown schematically in Fig. A-1, has proven to be very effective. On the basis of these trials the following procedure was adopted for the preparation of fine materials (38-62 microns).

1. To produce the fine specimens, all accumulated particles below 250μ, plus some of the crushed material, are divided into ~ 300-gram loads. Then one charge is placed in the uppermost sieve of each of the following nests of sieves:

   Nest A - 500, 210, 125, 105, 74μ, pan

   Nest B - 420, 250, 177, 149, 88, 62, 38μ, pan.

   Both nests are placed in the Tyler shaker and sieved for 20 minutes. Each sieve is given a tap with a wooden mallet after 10 minutes, and again just before the end of the sieving period.

2. Nest A is separated at the 105μ sieve, and Nest B at 88μ sieve. Both nests are restacked and sieved for an additional 10 minutes with tapping applied every 5 minutes.

3. Material below the 88μ sieve and above the 38μ sieve is stored for washing. Particles below 38μ are stored for possible future use.

4. All remaining material is placed into two ball mill jars. Particles below 420μ are ground in a ball mill jar containing a charge of 1/4-inch stainless steel balls; larger particles are ground in the ball jar containing tungsten carbide balls. The milling time for the fine specimens, that has proven to yield best results, is 45 minutes. Steps 1, 2, and 3 are then repeated.

5. The 38-88μ range material obtained in steps 1, 2, and 3 is fractionated in the setup shown in Fig. A-1 to remove particles finer than 38μ and coarser than 62μ.

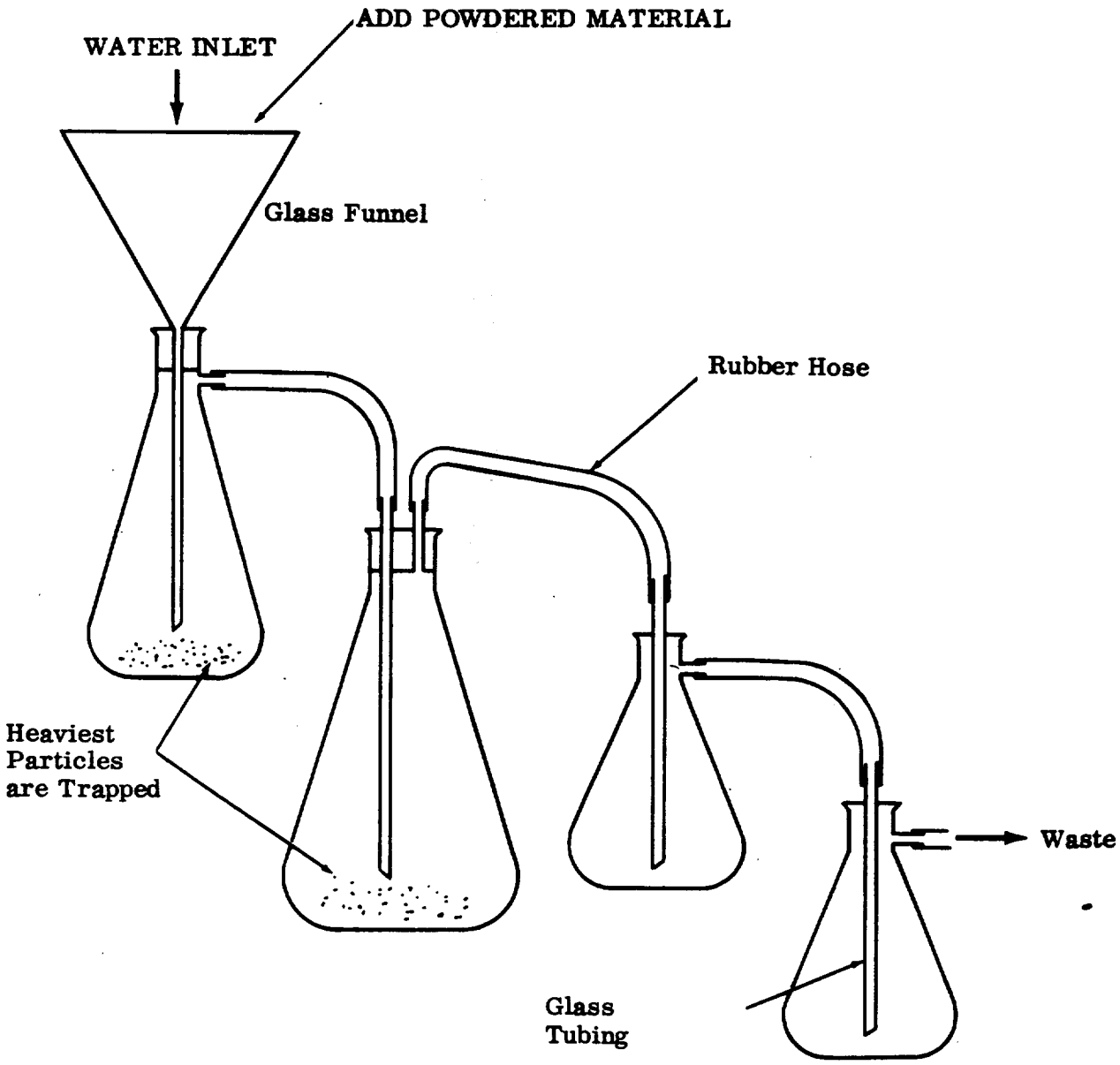

Flasks are Drawn in Their Proper Relative Positions

Fig. A-1 Fractionating Setup for Washing of Particles (38 - 62 μ)

APPENDIX B

OUTGASSING RATES OF MINERAL POWDERS

Difficulties in pumping down the vacuum systems, when mineral specimens taken off the shelf were placed inside the chambers, made it necessary to measure outgassing rates for basalt and quartz powders in the particle size ranges specified by the contract. The powders were placed inside a small container and baked between 5 and 7 hours at approximately 350°C. Due to the very high outgassing rates during the baking cycle, the ion pumps of the system had to be valved off; i.e., only the sorption pumps could be used during baking. Consequently, the pressure was never lower than 5×10^{-3} torr during this part of the baking. At the completion of baking, the sample container was air-cooled by means of two blowers. After approximately 1/2 hour, the container walls were at room temperature. Then the ion pump valve was slowly opened, the sorption pump closed as soon as the ion pumps indicated that they functioned normally, and the pump-down continued until an equilibrium pressure was reached.

The results of this outgassing is illustrated in Fig. B-1. First, a pump-down of the empty sample container is performed to establish curve I. Curves II and III are established by recording the pressure evolution of the samples, beginning with the opening of the ion pump valve. The outgassing rate of the powders can now be calculated from the equation

$$q_i = \frac{\Delta p_i \cdot S}{w} \quad \left\{\frac{\text{torr-liter}}{\text{sec} \cdot \text{gms}}\right\}, \qquad \text{(B-1)}$$

where Δp_i and, consequently, q_i are functions of time,

wq_i = gas load due to the outgassing of 55 gms of the specimen material after i hours of pumping,

Δp_i = increase in pressure due to this gas load in torr, and

S = pumping speed in liters/second.

It is of course assumed that every gas molecule leaving the specimen is captured by the pump, and that the outgassing rate of the walls of the system is negligible. Typical values of outgassing rates during this part of the procedure are given in Table B-1.

Table B-1

OUTGASSING (ROOM TEMPERATURE)

Material and Particle Size	Time (hrs.)	Outgassing rate for 55 gms. of material
Basalt (250-500μ)	1	2.3×10^{-7} torr·liter/sec
Basalt (37-62μ)	1	2.3×10^{-4} torr·liter/sec
Quartz (250-500μ)	1	9.2×10^{-6} torr·liter/sec
Quartz (37-62μ)	1	1.1×10^{-5} torr·liter/sec

Note: During this part of the procedure, the sample is at room temperature (20-25°C).

During baking, the sorption pump was valved off at one-hour intervals and the pressure rise was observed over a period of one minute. Knowing the volume of the section of the system that was used during this operation, and assuming that all other contributions to the total gas load (i.e., outgassing from the walls, leaks, etc.) are negligible, the outgassing rates can then be calculated from

$$q_i = V \frac{dp}{dt} , \qquad (B-2)$$

where q_i is the outgassing rate of a 55-gm sample in torr-liter/second, and i the baking time in hours. Typical values of outgassing rates for some of the materials during this stage of the procedure are given in Table B-2.

Table B-2

OUTGASSING (~ 350°C)

Material and Particle Size	Baking Time (hrs.)	Pressure (torr)	Outgassing rate for 55 gms. of material
Basalt (37-62μ)	2/3	5×10^{-3}	2.9×10^{-1} torr·liter/sec
Basalt (37-62μ)	1	5×10^{-3}	8.0×10^{-2} torr·liter/sec
Basalt (37-62μ)	5-1/2	5×10^{-3}	2.2×10^{-2} torr·liter/sec
Quartz (37-62μ)	2	5×10^{-3}	8.25×10^{-2} torr·liter/sec
Quartz (37-62μ)	3	5×10^{-3}	5.25×10^{-2} torr·liter/sec
Quartz (37-62μ)	5	5×10^{-3}	2.25×10^{-2} torr·liter/sec
Quartz (250-500μ)	1	5×10^{-3}	1.45×10^{-1} torr·liter/sec
Quartz (250-500μ)	2	5×10^{-3}	5.25×10^{-2} torr·liter/sec
Quartz (250-500μ)	3	5×10^{-3}	1.05×10^{-2} torr·liter/sec
Quartz (250-500μ)	4	5×10^{-3}	3.0×10^{-3} torr·liter/sec

Note: During this part of the procedure, the sample temperature is approximately 350°C.